European Journal of Taxonomy 970: 175–202
https://doi.org/10.5852/ejt.2024.970.2757
ISSN 2118-9773
www.europeanjournaloftaxonomy.eu
2024 · Prebus M.M. *et al.*

Research article

urn:lsid:zoobank.org:pub:A24A4604-EDD9-4833-ABF9-2ECF388C4703

Temnothorax caryaluteus sp. nov. (Hymenoptera: Formicidae): a new ant species from the eastern United States

Matthew M. PREBUS [1], Nhi NGUYEN [2],
Grant Navid DOERING [3] & Douglas B. BOOHER [4]

[1,2,3] Social Insect Research Group, School of Life Sciences,
Arizona State University, 550 E Orange St., Tempe, AZ 85281, USA.
[1] Department of Integrative Taxonomy of Insects, Institute of Biology,
University of Hohenheim, Garbenstraße 30, 70599, Stuttgart, Germany.
[1] KomBioTa – Center for Biodiversity and Integrative Taxonomy Research,
University of Hohenheim and State Museum of Natural History,
Wollgrasweg 2, 70599 Stuttgart, Germany.
[4] USDA Forest Service Southeastern Research Station, Athens, Georgia, USA.

[*] Corresponding author: mprebus@gmail.com
[2] Email: nhih.ngu@gmail.com
[3] Email naviddio@gmail.com
[4] Email: Douglas.Booher@usda.gov

[1] urn:lsid:zoobank.org:author:1A6494C7-795E-455C-B66F-7F6C32F76584
[2] urn:lsid:zoobank.org:author:4E495A2D-6AAA-49BA-84BB-B0C2B2217008
[3] urn:lsid:zoobank.org:author:D3800453-782F-4308-9F3E-6091E6FFF81E
[4] urn:lsid:zoobank.org:author:7A3F478F-A5E8-484F-844E-89759F58EEF7

Abstract. Although the ant genus *Temnothorax* is broadly distributed, extremely diverse, and contains multitudes of undescribed species, discovering new *Temnothorax* species in the eastern United States is rare due to the high concentration of taxonomic effort on this region. Here, we recognize and describe a new species that has consistently been misidentified in museum collections as *Temnothorax ambiguus*, a common inhabitant of acorn shells and leaf litter. Unlike *T. ambiguus*, *T. caryaluteus* sp. nov. nests primarily in arboreal microhabitats, especially within dead branches on live *Carya* and *Quercus* trees. We compare the morphology of *T. caryaluteus* sp. nov. against the congeners with similar appearance *T. ambiguus* and *T. curvispinosus*, and delineate diagnostic characters for *T. caryaluteus* sp. nov. Moreover, we provide an updated key to the *Temnothorax* species of the eastern United States.

Keywords. Morphometry, cryptic species, *Carya*, *Quercus*.

Prebus M.M., Nguyen N., Doering G.N. & Booher D.B. 2024. *Temnothorax caryaluteus* sp. nov. (Hymenoptera: Formicidae): a new ant species from the eastern United States. *European Journal of Taxonomy* 970: 175–202. https://doi.org/10.5852/ejt.2024.970.2757

Introduction

With 501 extant species, the myrmicine ant genus *Temnothorax* Mayr, 1861 is diverse and ubiquitous in the Northern hemisphere, including the northern Neotropics and Afrotropics (Prebus 2015, 2017; Bolton 2024). Although often overlooked by the casual observer due to their small size and cryptic nesting habits (Beckers *et al.* 1989), the lab-hardiness of *Temnothorax* has facilitated the use of several species as model organisms for behavioral studies (Möglich *et al.* 1974; Cole 1981; Rüppell *et al.* 2001; Pratt *et al.* 2002; Foitzik *et al.* 2004). Among these is *Temnothorax curvispinosus* (Mayr, 1866) and its close relatives in the eastern United States, which are arguably among the most thoroughly studied ant species (Talbot 1957; Wilson 1974; Stuart 1985; Pratt & Pierce 2001; Linksvayer 2008; Herbers & Johnson 2007; Booher *et al.* 2017).

In the eastern United States, here defined as all states east of the Mississippi River, free-living *Temnothorax* species are often encountered nesting in acorns, hickory nuts, or in dead twigs in the leaf litter (*T. ambiguus* (Emery, 1895), *T. curvispinosus*, *T. longispinosus* (Roger, 1863), *T. torrei* (Aguayo, 1931), *T. tuscaloosae* (Wilson, 1951)). However, some species nest directly in the soil (*T. texanus* (Wheeler, 1903), *T. palustris* (Cover & Deyrup, 2004)), or are arboreal, nesting in dead branches on live trees, tree cavities, or under bark (*T. allardycei* (Mann, 1920), *T. bradleyi* (Wheeler, 1913), *T. schaumii* (Roger, 1863), *T. smithi* (Baroni Urbani, 1978)), while others are more ambivalent about nest locations (*T. pergandei* (Emery, 1895)).

Other eastern United States species are social parasites, such as *Temnothorax americanus* (Emery, 1895), *T. duloticus* (Wesson, 1937), *T. minutissimus* (Smith, 1942), and *T. pilagens* Seifert *et al.*, 2014. These latter three social parasites, along with their most common hosts (*T. ambiguus*, *T. curvispinosus*, and *T. longispinosus*), comprise most of the *T. longispinosus* species group (Prebus 2017, 2021), which has been the subject of extensive studies on social parasitism (Blatrix & Herbers 2004; Foitzik *et al.* 2004; Beibl *et al.* 2005; Achenbach & Foitzik 2009; Jongepier *et al.* 2015).

Here, we describe all castes of a new widespread free-living arboreal *Temnothorax longispinosus* group species from the eastern United States, which has been frequently misidentified as *T. ambiguus* in collections. Despite its superficial resemblance to *T. ambiguus*, *T. caryaluteus* sp. nov. is more closely related to *T. curvispinosus* (Prebus in prep.). Furthermore, we include diagnostic characteristics to separate gynes of *T. caryaluteus* sp. nov. from lookalike species, and a revised key to workers of all *Temnothorax* species from the eastern United States.

Material and methods

This study is based on the examination of 343 workers, 38 gynes, and 10 males, with measurements taken from 138 specimens: 107 workers, 23 gynes, and 8 males. We compared three species that are most likely to be confused with each other: *Temnothorax ambiguus*, *T. curvispinosus*, and *T. caryaluteus* sp. nov. All measurements and morphological observations in this study were performed at a maximum magnification of 160× using a Leica M205C stereo microscope, a movable stage equipped with orthogonal digital micrometers, and an ocular graticule. The images used in this study were taken at a maximum magnification of 160× with a Leica DFC450 digital camera mounted on a Leica M205C stereo microscope using the Leica Application Suite ver. 4.5 (Leica, Wetzlar, Germany). Images were z-stacked using the program HeliconFocus ver. 6.7.1 (HeliconSoft, Kharkiv, Ukraine). All measurements in this study are expressed in millimeters, up to three decimal places. The measurements in the taxon treatment are presented as ranges, from minimum to maximum, with the arithmetic mean following the range in parentheses. Many of the following morphological measurements are based on Seifert & Csősz (2015) and Csősz & Fisher (2015). See Fig. 1 for an illustration of the measurements listed below.

SL = Scape length. Maximum scape length excluding the basal neck and the articular condyle (Fig. 1c).

EL = Maximum diameter of the compound eye (Fig. 1a).

EW = Minimum diameter of the compound eye (Fig. 1a).

FRS = Frontal carina distance. Distance between the frontal carinae immediately caudal of the posterior intersection points between frontal carinae and torular lamellae. If these dorsal lamellae do not laterally surpass the frontal carinae, the deepest point of scape corner pits may be taken as the reference line. These pits take up the inner corner of the scape base when the scape is directed fully caudally and produces a dark, triangular shadow in the lateral frontal lobes immediately posterior to the dorsal lamellae of the scape joint capsule (Fig. 1c).

CW = Maximum width of the head, including the compound eyes (Fig. 1c).

CWb = Maximum width of head capsule without the compound eyes, measured posterior to the eyes (Fig. 1c).

CL = Maximum cephalic length. The head must be carefully tilted into full face view, providing the true maximum. If excavations of the posterior margin of the head capsule and/or anterior margin of the clypeus are present, then the measurement is taken from an imaginary line that spans the excavations from the posterior- or anterior-most margins (Fig. 1c).

PoOC = Postocular distance. Adjust the head to the measuring position of CL. Using an ocular graticule, PoOC is the length between posterior margin of the compound eyes and the posterior margin of the head capsule. If the posterior margin of the head capsule is excavated, then the measurement is taken from an imaginary line that spans the excavation from the posterior-most margins (Fig. 1c).

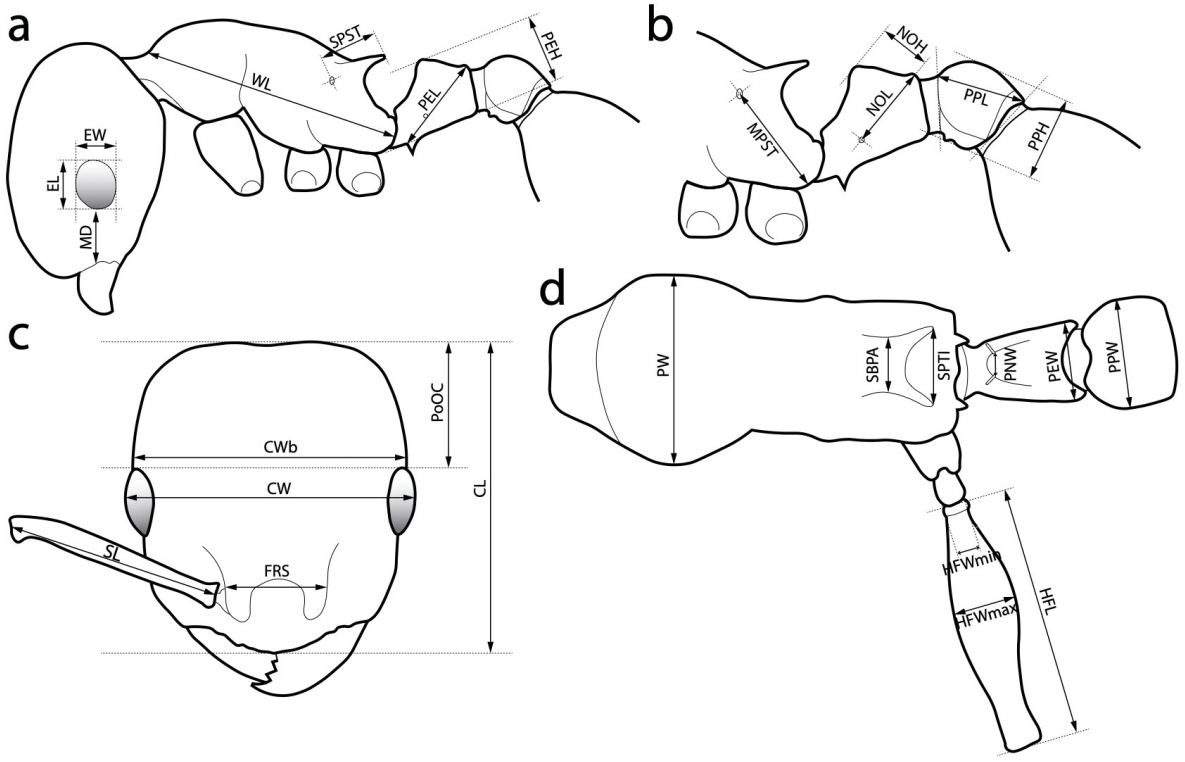

Fig. 1. Measurements used in this study. **a**. Profile view. **b**. Profile view detail. **c**. Full face view. **d**. Dorsal view, excluding head and gaster.

MD = Malar distance. Minimum distance from the anterior margin of the compound eye to where the mandible articulates with the head capsule (Fig. 1a).

WL = Weber's length. Distance between the caudalmost point of propodeal lobe to the inflection point between the pronotal neck and the pronotal declivity (Fig. 1a).

SPST = Propodeal spine length. Distance between the center of the propodeal spiracle and the tip of the propodeal spine (Fig. 1a).

MPST = Maximum distance from the center of the propodeal spiracle to the posteroventral corner of the ventrolateral margin of the metapleuron (Fig. 1b).

PEL = Petiole length. Diagonal petiolar length in lateral view; measured from the apex of the subpetiolar process to the posterodorsal corner of caudal cylinder (Fig. 1a).

NOL = Petiolar node length. Measured in lateral view from the center of the petiolar spiracle to an imaginary line that joins the posterodorsal and posteroventral corners of the caudal cylinder (Fig. 1b).

NOH = Petiolar node height. Maximum height of the petiolar node, measured in lateral view from the uppermost point of the petiolar node perpendicular to a reference line set from the petiolar spiracle to the imaginary midpoint of the transition between the dorso-caudal slope of the node and dorsal profile of caudal cylinder of the petiole (Fig. 1b).

PPL = Postpetiole length. The longest distance, perpendicular to the posterior margin of the postpetiole, between the posterior postpetiolar margin and the anterior postpetiolar margin, excluding the helcium (Fig. 1b).

PEH = Petiole height. The longest distance measured from the ventral petiolar profile at node level (perpendicular to the chord length of the petiolar sternum, excluding the subpetiolar process) to the distalmost point of the dorsal profile of the petiolar node (Fig. 1a).

PPH = Maximum height of the postpetiole in lateral view measured perpendicularly to a line defined by the linear section of the segment border between postpetiolar tergite and sternite (Fig. 1b).

PW = Pronotum width. Maximum width of the pronotum in dorsal view (Fig. 1d).

SBPA = Minimum propodeal spine distance. The smallest distance of the lateral margins of the propodeal spines at their base. This should be measured in antero-dorsal view: the wider parts of the ventral propodeum do not interfere with the measurement in this position. If the lateral margins of propodeal spines diverge continuously from the tip to the base, a smallest distance at base is not defined. In this case, SPBA is measured at the level of the bottom of the interspinal meniscus (Fig. 1d).

SPTI = Apical propodeal spine distance. The distance of propodeal spine tips in dorsal view; if spine tips are rounded or truncated, the centers of spine tips are taken as reference points (Fig. 1d).

PNW = Width of petiolar node in dorsal view, using the anterior pair of node setae as anchor points (Fig. 1d).

PEW = Maximum width of petiole in dorsal view, measured across the widest point of the caudal cylinder (Fig. 1d).

PPW = Postpetiole width. Maximum width of postpetiole in dorsal view (Fig. 1d).

HFL = Hind femur length. Maximum length of the metafemur in dorsal view (Fig. 1d).

HFWmax = Maximum metafemur width in dorsal view (Fig. 1d).

HFWmin = Minimum metafemur width in dorsal view, taken at the point of articulation with the trochanter (Fig. 1d).

CS = Absolute cephalic size. The arithmetic mean of CL and CWb.

ES = Absolute eye size. The arithmetic mean of EL and EW.

SI = Scape index: SL/CWb × 100.

EI = Eye index: EL/CWb × 100.

CI = Cephalic length index: CWb/CL × 100.

WLI = Weber's length index: WL/CWb × 100.
SBI = Propodeal spine base index: SBPA/CWb × 100.
PSI = Propodeal spine length index: SPST/WL × 100.
PWI = Postpetiole width index: PPW/PEW × 100.
PLI = Petiole length index: PEL/PPL × 100.
NI = Petiolar node shape index: NOL/NOH × 100.
PNWI = Petiolar node width index: PNW/PEW × 100.
NLI = Petiolar node length index: NOL/PEL × 100.
FI = Metafemur width index: HFWmax/HFWmin × 100.
FRSI = Frontal carina distance index: FRS/CWb × 100.
SPTII = Apical propodeal spine distance index: SPTI/CWb × 100.

Collection and raw measurement data for all specimens used in this study can be found in Supp. file 1 and Supp. file 2, respectively. We mapped the distributions of *Temnothorax ambiguus*, *T. curvispinosus*, and *T. caryaluteus* sp. nov. with R ver. 4.1.3 (R Core Team 2022) using the collection data of all physical specimens examined in this study and script adapted from Prebus (2021). To supplement our distribution data, we examined photographs posted on BugGuide.net and iNaturalist.org. To make determinations and decide whether to include records, we used only photographs of workers where the propodeal spines, a key diagnostic character, were observable. We estimated coordinates for observations from BugGuide.net based on locality data associated with the records. Records of these observations, along with the associated URLs, are included in Supp. file 1.

Morphometric analysis

Means of raw morphological measurements and indices of *Temnothorax ambiguus*, *T. curvispinosus*, and *T. caryaluteus* sp. nov. were compared with the pairwise Wilcoxon rank-sum test using a custom R script and the package 'ggpubr' (Kassambara 2023; see Dryad for data and script: https://doi.org/10.5061/dryad.tb2rbp08q; Prebus *et al.* 2024); overall significance for each set of comparisons was calculated using the Kruskal-Wallis test.

Repositories

Specimens have been deposited in the following repositories:
ABS = Archbold Biological Station, Lake Placid, Florida, USA
ASUHIC = Hasbrouck Insect Collection, Arizona State University, Tempe, Arizona, USA
CASC = California Academy of Sciences, San Francisco, California, USA
LACM = Natural History Museum of Los Angeles, Los Angeles, California, USA
MCZC = Museum of Comparative Zoology, Harvard University, Cambridge, Massachusetts, USA
MEM = Mississippi State University, Mississippi State, Mississippi, USA
MMPC = Matthew M. Prebus personal collection, Arizona State University, Tempe, Arizona, USA
MSNG = Natural History Museum, Genoa, Italy
NHMUK = Natural History Museum, London, United Kingdom
SMNG = Staatliches Museum für Naturkunde Görlitz, Görlitz, Germany
UCDC = Bohart Museum of Entomology, University of California Davis, Davis, California, USA
UGCA = University of Georgia Collection of Arthropods, Athens, Georgia, USA
USNM = National Museum of Natural History, Washington D.C., USA
UTIC = University of Texas Insect Collection, Austin, Texas, USA
VMNH = Virginia Museum of Natural History, Martinsville, Virginia, USA

Results

Morphometric analysis

We found that workers of *Temnothorax caryaluteus* sp. nov. are consistently distinguishable from those of *Temnothorax ambiguus* based on the smaller ratio of the width of the petiolar node to the overall petiole in dorsal view (PNWI 41.6–58.6 vs 65.7–92.5; Fig. 2a) and the distance between the tips of the propodeal spines in dorsal view (SPTII 21.9–31.8 vs 35.8–49.9; Fig. 2c). Additionally, *Temnothorax caryaluteus* is distinguishable from *T. curvispinosus* by the length of the propodeal spine in profile view (PSI 18.6–26.1 vs 31.5–42.7; Fig. 2b).

The gyne of the new species is difficult to separate from those of *T. ambiguus* and *T. curvispinosus*, but our analyses indicate that they are readily separated by several characters: the smaller ratio of the width of the petiolar node to the overall petiole in dorsal view separates *T. caryaluteus* sp. nov. from *T. ambiguus* (PNWI 51.3–58.8 vs 62.9–82.0; Fig. 3a); the relatively smaller eyes separate *T. caryaluteus* from both *T. curvispinosus* and *T. ambiguus* (EI 35.3–37.0 vs 38.7–42.3 and 37.5–40.4, respectively; Fig. 3b); the more closely approximated propodeal spine tips separate *T. caryaluteus* from *T. ambiguus* (SPTII 32.0–34.5 vs 39.0–47.6; Fig. 3c). The means of several other measurements and indices were

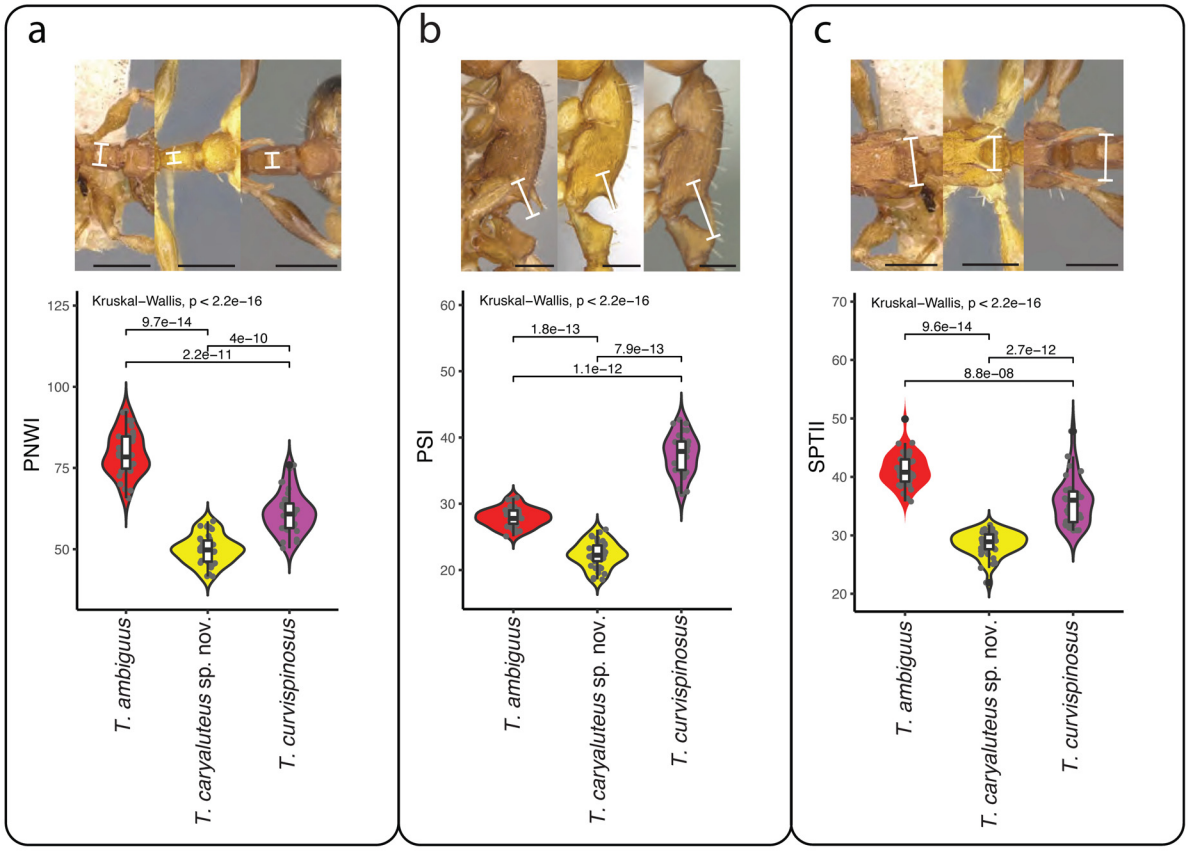

Fig. 2. Illustrations of characters measured on *Temnothorax* worker specimens (top) compared with worker morphometric analysis results (bottom). **a**. Petiolar node width index (PNWI). **b**. Propodeal spine distance (PSI). **c**. Apical propodeal spine distance index (SPTII). Photographs of *T. ambiguus* by Will Ericson (MSNG, CASENT0904763; from antweb.org); photographs of *T. curvispinosus* by April Nobile (ABS, CASENT0104040; from antweb.org); photographs of *T. caryaluteus* sp. nov. by Matthew Prebus (holotype, USNM, CASENT4011115). Scale bars 0.2 mm.

significantly different between species, but their distributions overlapped to varying degrees (Supp. file 3, Supp. file 4). Below, we describe *Temnothorax caryaluteus* from the eastern United States, an apparently common but historically misidentified species.

Taxonomy

Class Insecta Linnaeus, 1758
Order Hymenoptera Linnaeus, 1758
Suborder Apocrita Latreille, 1810
Family Formicidae Latreille, 1809
Subfamily Myrmicinae Lepeletier de Saint-Fargeau, 1835
Tribe Crematogastrini Forel, 1893
Genus *Temnothorax* Mayr, 1861

Temnothorax caryaluteus sp. nov.
urn:lsid:zoobank.org:act:71800550-6BD3-475F-B7BC-D5C0BBF15686
Fig. 4

Diagnosis

Among the species of the eastern United States, the worker of *Temnothorax caryaluteus* sp. nov. is distinguishable by the following combination of characters: antennae 11-segmented; antennal scrobe absent; mandible with five masticatory teeth; antennal scape long: when fully retracted, failing to reach the posterior margin of the head by < 2 times the width of the antennal scape; subpetiolar process absent or weakly developed; propodeal spines shorter than, or as long as, the propodeal declivity in profile view, varying from as long as broad to twice as long as broad at the base; dorsum of mesosoma sculptured; workers > 3 mm in length; head, mesosoma, and gaster integument light colored (often yellowish-orange), with the posterior half of the first gastral tergite infuscated; propodeal spines closely approximated, their bases separated by roughly the length of the propodeal spine in dorsal view, their union forming a U-shape; apex of petiolar node acute to narrowly rounded in profile view, about as half as wide as the petiole in dorsal view; mesosoma slightly arched in profile view. Free-living (non-parasitic) species; nests under bark and in dead branches and twigs of live trees.

Etymology

The name *caryaluteus* is a portmanteau of ancient Greek *carya* ("walnut", the genus name for hickory) and the Latin *luteus* ("yellow"). This name was proposed by Brodie Gaudie as the result of an outreach project conducted by the authors in coordination with the United States Forest Service, in which several elementary school classes partook in a workshop focused on the practice of taxonomy and its underlying philosophy. Names for the new species were proposed by classrooms and individuals and were subsequently voted on in a social media campaign.

Type material examined

Holotype

USA – **Kentucky** • ☿; Whitley County, Williamsburg; 36.739° N, 84.168° W ± minute; 320 m a.s.l.; 27 Jul. 2015; M. Deyrup#ANTC43885; in fallen branch of *Carya illinoiensis*; USNM, CASENT4011115.

Paratypes

USA – **Kentucky** • 1 dealate ♀; same data as for holotype; USNM, CASENT4011128 • 3 ☿☿; same data as for holotype; USNM, CASENT4011123 to CASENT4011125 • 3 ☿☿; same data as for holotype; USNM, CASENT4011141 to CASENT4011143 • 2 ☿☿; same data as for holotype; ABS, CASENT0759059 to CASENT0759060 • 2 ☿☿; same data as for holotype; ASUHIC, CASENT4011121

to CASENT4011122 • 2 ☿☿; same data as for holotype; CASC, CASENT0759057 to CASENT0759058 • 6 ☿☿; same data as for holotype; MCZC, CASENT4011106 to CASENT4011111 • 2 ☿☿; same data as for holotype; MEM, CASENT0759052 to CASENT0759053 • 3 ☿☿; same data as for holotype; UGCA, CASENT4011112 to CASENT4011114 • 5 ☿☿; same data as for holotype; UGCA, CASENT4011116 to CASENT4011120 • 2 ☿☿; same data as for holotype; UTIC, CASENT0759054 to CASENT0759055 • 2 ☿☿; same data as for holotype; VMNH, CASENT4011104 to CASENT4011105.

Non-type material examined

USA – **Alabama** • 1 dealate ♀; Madison County, 2.3 miles SE of Gurley; 34.0158° N, 86.33611° W; 295 m a.s.l.; 10 Jun. 2018; S.Y. Wang#ANTC46095; by pasture; UV-light/sheet; MEM, MEM238160. – **Arkansas** • 1 ☿; Newton County, Buffalo National River, Steel Creek; 36.038853° N, 93.33729° W; 300 m a.s.l.; 9 Oct. 2009; M. Skvarla and R. Fisher#ANTC46096; MEM, MEM241251. – **Georgia** • 1 ☿; Clarke County, Sandy Creek Nature Center; 33.98683° N, 83.38283° W ± minute; 205 m a.s.l.; 30 Apr. 2012; D. Booher#DBB234W; UGCA, CASENT0750495 • 2 ☿☿; Whitfield County, near Pinhoti trail crossing on access road; 34.739° N, 85.0167° W ± 50 m; 432 m a.s.l.; 30 Mar. 2012; D. Booher#DBBC5000; hardwood forest, chestnut oak: fork of dead branch on live tree; UGCA, CASENT0749972 to CASENT0749973 • 3 ☿☿; same data as for preceding; D. Booher#DBBC5000b; UGCA, CASENT0749974 to CASENT0749976 • 6 ☿☿; same data as for preceding; UGCA,

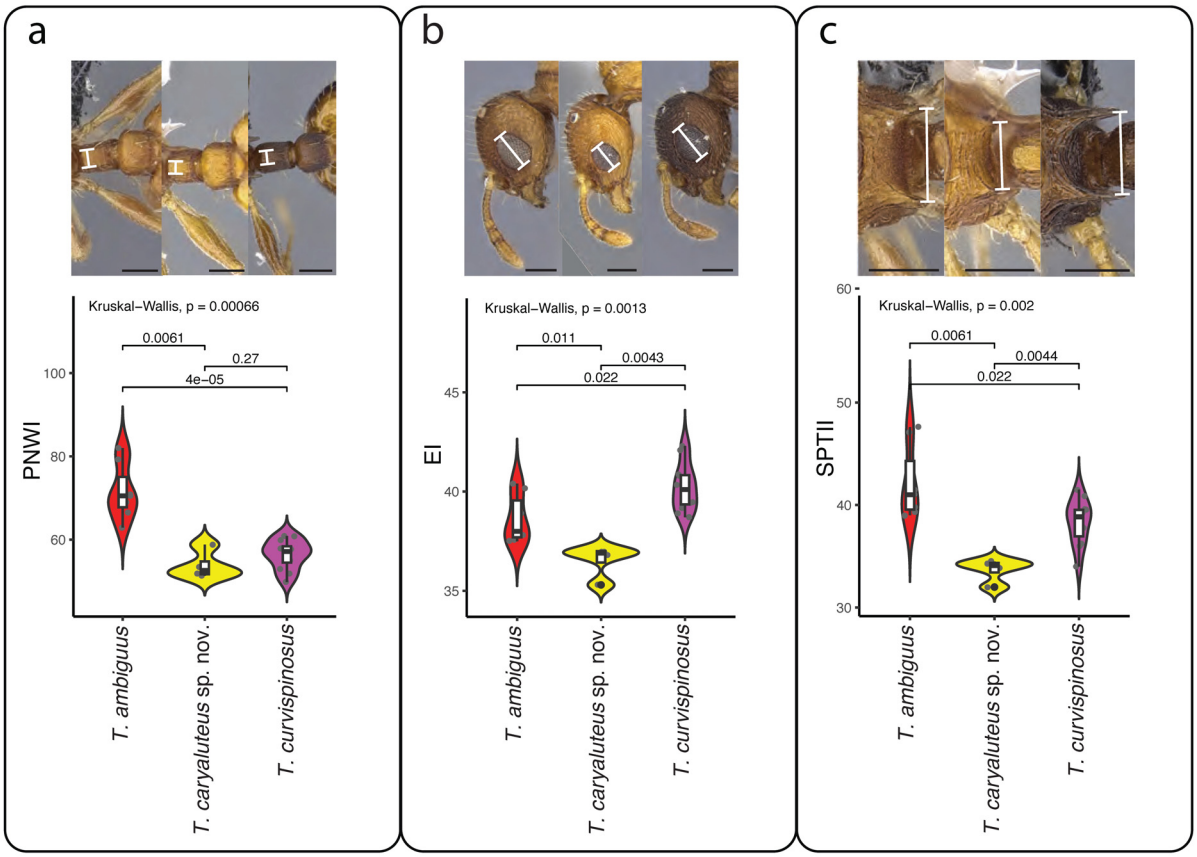

Fig. 3. Illustrations of characters on measured on *Temnothorax* gyne specimens (top) compared with gyne morphometric analysis results (bottom). **a**. Petiolar node width index (PNWI). **b**. Eye length index (EI). **c**. Apical propodeal spine distance index (SPTII). All photographs by Matthew Prebus (*T. ambiguus*: INHS, CASENT0759703; *T. curvispinosus*: MMPC, CASENT0755051; *T. caryaluteus* sp. nov., paratype: USNM, CASENT4011128). Scale bars 0.2 mm.

CASENT0749978 to CASENT0749983. – **Indiana** • 1 dealate ♀; Dubois County, Jasper; 38.391442° N, 86.931109° W ± 5 km; 150 m a.s.l.; 28 Feb. 2021; J. Ruhe#ANTC46158; lab colony, reared from queen collected at blacklight; MMPC, CASENT4010186 • 1 ☿; same data as for preceding; MMPC, CASENT4010185 • 1 ☿; same data as for preceding; 18 Mar. 2021; J. Ruhe#ANTC46159; MMPC, CASENT4010187 • 2 ♂♂; Monroe County, Bloomington, Griffey Lake Nature Preserve; 39.205833° N, 86.525278° W; 230 m a.s.l.; 10 Jun. 2024; G. Doering#GLTca1; oak-hickory forest, under bark of downed tree; MMPC, CASENT4012894, CASENT4012904 • 2 ☿☿; same data as for preceding; MMPC, CASENT4012895, CASENT4012897 • 1 ♂; same data as for preceding; USNM, CASENT4012896 • 1 ♂; same data as for preceding; ABS, CASENT4012898 • 1 ♂; same data as for preceding; UGCA, CASENT4012899 • 1 ♂; same data as for preceding; ASUHIC, CASENT4012900 • 1 ♂; same data as for preceding; CASC, CASENT4012901 • 1 ♂; same data as for preceding; MCZC, CASENT4012902 • 1 ♂; same data as for preceding; MEM, CASENT4012903. – **Kentucky** • 1 ☿; Whitley County, Williamsburg; 36.743418° N, 84.159654° W ± minute; 300 m a.s.l.; 25 Jun. 2017; M. Deyrup#ANTC43836; emerged from dead branch *Carya illinoiensis*; ABS, CASENT0758863 • 2 ☿☿; same data as for preceding; ABS, CASENT4011101 to CASENT4011102 • 1 ♀; same data as for preceding; ABS, CASENT4011100 • 1 ♀; same data as for preceding; ABS, CASENT4011103 • 1 ☿; same data as for preceding; 36.739° N, 84.168° W ± minute; 320 m a.s.l.; 27 Jul. 2015; M. Deyrup#ANTC43883; branch of *Carya illinoiensis*; ABS, CASENT0759047 • 4 ☿☿; same data as for preceding; 16 Mar. 2015; M. Deyrup#ANTC43884; in dead branch of *Carya illinoiensis*; ABS, CASENT0759048 to CASENT0759051 • 9 ☿☿; same data as for preceding; ABS, CASENT4011129 to CASENT4011137 • 23 ☿☿; same data as for preceding; 27 Jul. 2015; M. Deyrup#ANTC43887; branch of *Carya illinoiensis*; ABS, CASENT0759061-5, CASENT4011138-55. – **Mississippi** • 1 ☿; DeSoto County, 1 mile north of Handy Corner; 34.978889° N, 89.742222° W; 120 m a.s.l.; 18 Aug. 2005; A.B. Edwards#ANTC46097; Lindgren funnel trap baited with Typosan and alpha-pinene; MEM, MEM241880 • 1 ☿; Lee County, Natchez Trace, mile 273; 34.406111° N, 88.6375° W; 125 m a.s.l.; 27 May 2003; T.L. Schiefer and J.A. MacGown#ANTC46098; deciduous forest, Lindgren funnel trap; MEM, MEM241875 • 1 ☿; Madison County, Natchez Trace Parkway; 32.654167° N, 89.778056° W; 115 m a.s.l.; 10 Jul. 2002; M. Allred and K. Lewis#ANTC46099; Lindgren funnel trap; MEM, MEM241881 • 1 ☿; Marshall County, Wall Doxey State Park; 34.661389° N, 89.465556° W; 110 m a.s.l.; 15 May 2006; A.B. Edwards#ANTC46100; Lindgren funnel trap baited with Typosan; MEM, MEM241878. – **Missouri** • 1 ☿; Barry County, Roaring River State Park; 36.58559° N, 93.836411° W ± 1 km; 315 m a.s.l.; 27 Jun. 1995; A.L. Wild#ANTC46161; man-modified "lawn" near parking lot; UTIC, UTIC219525 • 1 ☿; same data as for preceding; UTIC, UTIC204575. – **Virginia** • 1 ☿; Shenandoah County, near Elizabeth Furnace Campground; 38.94978102° N, 78.299409° W ± 3 m; 210 m a.s.l.; 24 May 2015; M.M. Prebus#MMP1896; riparian mixed hardwood forest, nest in dead standing wood; MMPC, CASENT0755055 • 1 ☿; same data as for preceding; M.M. Prebus#MMP1897; MMPC, CASENT0755056 • 1 ☿; same data as for preceding; 38.94893202° N, 78.29862496° W ± 3 m; 215 m a.s.l.; 24 May 2015; M.M. Prebus#MMP1899; riparian mixed hardwood forest, single worker in dead branch on live tree; MMPC, CASENT0755063.

Description

Worker

Measurements and indices (n = 38): SL = 0.345–0.476 (0.428); FRS = 0.153–0.25 (0.205); CW = 0.484–0.616 (0.572); CWb = 0.442–0.586 (0.532); PoOC = 0.201–0.267 (0.240); CL = 0.515–0.642 (0.598); EL = 0.104–0.156 (0.133); EW = 0.079–0.113 (0.097); MD = 0.104–0.186 (0.142); WL = 0.567–0.757 (0.690); SPST = 0.115–0.181 (0.153); MPST = 0.17–0.241 (0.212); PEL = 0.217–0.288 (0.263); NOL = 0.11–0.172 (0.146); NOH = 0.039–0.11 (0.086); PEH = 0.149–0.216 (0.191); PPL = 0.129–0.202 (0.163); PPH = 0.134–0.185 (0.164); PW = 0.288–0.387 (0.349); SBPA = 0.067–0.13 (0.101); SPTI = 0.103–0.174 (0.152); PEW = 0.123–0.166 (0.140); PNW = 0.052–0.085 (0.070); PPW = 0.156–0.214 (0.194); HFL = 0.361–0.514 (0.460); HFWmax = 0.093–0.132 (0.118); HFWmin = 0.037–0.056 (0.046);

CS = 0.489–0.612 (0.565); ES = 0.093–0.132 (0.115); SI = 73.7–89 (80.6); EI = 21.5–28.5 (24.9); CI = 82.6–100.2 (88.9); WLI = 120–142 (130); SBI = 14.3–22.7 (19.0); PSI = 18.6–26.1 (22.3); PWI = 122–152 (138); PLI = 123–192 (163); NI = 138–290 (177); PNWI = 41.6–58.6 (49.9); NLI = 42.6–64.2 (55.7); FI = 222–300 (258); FRSI = 30.8–46.7 (38.6); SPTII = 21.9–31.8 (28.5).

In full face view, head subquadrate, often longer than broad (CI 82.6–100.2). Mandibles weakly, finely striate but shining and armed with five teeth: the apical-most well developed and acute, followed by a less developed preapical tooth and three equally developed smaller teeth. Anterior clypeal margin convex. Antennal scapes short: when fully retracted, failing to reach the posterior margin of the head capsule by about the two times the maximum width of the scape (SI 73.7–89). Antennae 11-segmented; antennal club of composed of three segments, with the apical-most segment about the same length as the preceding two in combination. Frontal carinae short, extending past the antennal toruli by about two times the maximum width of the antennal scape. Compound eyes weakly protruding past the lateral margins of the head capsule. Lateral margin of head very weakly convex above the compound eyes to the posterior margin of the head, slightly constricted below the compound eyes to the mandibular insertions. Posterior head margin weakly concave medially, rounding evenly into the lateral margins.

In profile view, compound eyes elongate-ovular and small (EI 21.5–28.5), with 10 ommatidia in longest row. Pronotal declivity indistinct, neck and anterior face of pronotum forming a ~120° angle. Mesosoma arched: evenly convex from where it joins the pronotal neck to propodeal spines. Promesonotal suture extending from the posterior margin of the procoxal insertion to the mesothoracic spiracle, which is moderately well developed, then continuing dorsally as a weak disruption of the integument sculpture. Metanotal groove visible as a weak disruption of the sculpture laterally from where it arises between the mid- and hind coxae to the poorly developed metathoracic spiracle, which is nearly indistinguishable against the ground sculpture, then continuing dorsally as a weak disruption of the integument sculpture. Propodeal spiracle weakly developed, directed posterolaterally, and separated from the propodeal declivity by about three spiracle diameters. Propodeal spines short (PSI 18.6–26.1), about two thirds the length of the propodeal declivity, tapering evenly from the base, slightly curved, and acute. Propodeal declivity weakly concave, forming a rounded ~100° angle with the base of the propodeal spines. Propodeal lobes rounded and weakly developed. Metapleural gland bulla small, extending from the metacoxal insertion halfway to the propodeal spiracle. Petiole short (PLI 123–192), with tubercles anterodorsally. Subpetiolar process in the form of a small, acute, triangular tooth which grades evenly into the ventral margin of the petiole posteriorly; ventral margin of petiole flat to weakly concave posterior to it. Petiolar peduncle short: comprising less than a quarter of the total petiole length. Petiolar node erect and cuneiform to slightly rounded: peduncle grading evenly into the anterior node face; anterior face forming a ~90° angle with the flat posterior face; posterior face forms a ~120° angle with the caudal cylinder. Postpetiole rounded anteriorly, anterior face rounds evenly into the dorsal face; weakly lobed ventrally.

In dorsal view, humeri developed and distinct: evenly rounded and wider than the rest of the mesosoma; mesothoracic spiracles weakly protruding past the lateral margins of the mesosoma, visible as slight angles where the pronotum meets the mesonotum. Promesonotal groove visible as a disruption in the ground sculpture. Metanotal groove visible as a disruption in the ground sculpture. Propodeal spines closely approximated basally and diverging apically, their apices separated from each other by about twice their length, the negative space between them "V"-shaped. Petiolar peduncle with spiracles weakly protruding past the lateral margins. Petiolar node, when viewed at a posterodorsal aspect, tapering evenly from the base, with the dorsal margin evenly convex; apex of node narrower than the peduncle and caudal cylinder. Postpetiole narrow (PWI 122–152) and campaniform. Anterior margin of the postpetiole evenly rounds into the lateral margins; lateral margins parallel to the rounded posterior corners; posterior margin notched. Metafemur weakly to moderately incrassate (FI 222–300).

Sculpture: median clypeal carina absent, remainder with longitudinal rugulae. Lateral clypeal lobes with additional rugulae; ground sculpture smooth. Antennal scapes weakly sculptured. Cephalic dorsum predominantly areolate, with the slightly longitudinally elongate areolae arranged into longitudinal rows by fine costulae; very fine concentric rugulae surrounding the antennal insertions. Lateral surfaces of head sculptured similarly to the dorsum, becoming smooth behind the compound eyes; fine rugose sculpture overlying the areolate sculpture between the compound eye and mandibular insertion. Ventral surface of head mostly smooth and shining. Pronotal neck and anterior face of the pronotum areolate. Lateral surface of the pronotum longitudinally rugose. Meso- and metapleurae areolate, with fine costulae overlying the ground sculpture. Smooth and shining with weak areolae between the propodeal spiracle and the propodeal spines. Dorsal surface of pronotum longitudinally rugose, becoming anastomosed anteriorly. Dorsal face of the mesonotum smooth and shining. Dorsal face of propodeum rugose. Femora shining. Petiole predominantly areolate; anterior face of petiolar node smooth and shining. Postpetiole predominantly areolate; anterior face smooth and shining. First gastral tergite and sternite smooth and shining, without spectral iridescence.

Setae: antennal scapes and funiculi with short, decumbent pilosity. Dorsum of the head, pronotum, waist segments, and gaster with moderately abundant, erect, blunt-tipped setae, the longest of which are about the width of the compound eye. The head bears ~28, mesosoma ~14, petiole 4, postpetiole ~6, and first gastral tergite ~26 setae.

Color: predominantly orange-yellow, with the posterior margin of the first gastral tergite slightly infuscated.

Gyne

Measurements and indices (n = 4): SL = 0.429–0.455 (0.440); FRS = 0.219–0.237 (0.228); CW = 0.655–0.688 (0.671); CWb = 0.597–0.654 (0.618); PoOC = 0.231–0.247 (0.239); CL = 0.622–0.677 (0.643); EL = 0.221–0.231 (0.226); EW = 0.175–0.189 (0.182); MD = 0.102–0.116 (0.108); WL = 1.014–1.051 (1.029); SPST = 0.136–0.164 (0.149); MPST = 0.243–0.276 (0.260); PEL = 0.329–0.358 (0.344); NOL = 0.179–0.18 (0.180); NOH = 0.13–0.137 (0.134); PEH = 0.238–0.256 (0.247); PPL = 0.179–0.194 (0.189); PPH = 0.212–0.237 (0.226); PW = 0.576–0.595 (0.585); SBPA = 0.245–0.26 (0.253); SPTI = 0.205–0.211 (0.208); PEW = 0.191–0.195 (0.194); PNW = 0.1–0.114 (0.104); PPW = 0.25–0.274 (0.260); HFL = 0.531–0.562 (0.545); HFWmax = 0.127–0.136 (0.131); HFWmin = 0.048–0.058 (0.051); CS = 0.616–0.666 (0.631); ES = 0.198–0.210 (0.204); SI = 69.6–73.2 (71.2); EI = 35.3–37.0 (36.5); CI = 93.4–100.0 (96.1); WLI = 161–173 (167); SBI = 39.8–41.9 (40.9); PSI = 13.2–15.6 (14.4); PWI = 128–141 (134.199); PLI = 176–185 (182); NI = 131–138 (134); PNWI = 51.3–58.8 (53.8); NLI = 50.3–54.4 (52.2); FI = 234–271 (258); FRSI = 36.2–37.7 (36.9); SPTII = 32.0–34.5 (33.7).

In full face view, head subquadrate (CI 93.4–100.0). Mandibles weakly striate but shining and armed with five teeth: the apical-most well developed, followed by a less developed preapical tooth and three equally developed smaller teeth. Anterior clypeal margin evenly convex medially. Frontal carinae moderately long, extending past the antennal toruli by about four times the maximum width of the antennal scape. Antennal scapes short: when fully retracted, failing to reach the posterior margin of the head capsule by about three times the maximum width of the scape (SI 69.6–73.2). Antennae 11-segmented; antennal club composed of three segments, with the apical-most segment about as long as the preceding two in combination. Compound eyes protruding past the lateral margins of the head capsule. Lateral margins of head evenly convex behind the compound eyes, then parallel to each other from the mandibular insertions to below the compound eyes. Posterior head margin flat, rounding evenly into the lateral margins.

In profile view, compound eyes ovular and large (EI 35.3–37.0), with 15 ommatidia in longest row. Mesoscutum rounded evenly anteriorly, covering the dorsal surface of the pronotum, and flat dorsally. Mesoscutellum slightly lower than the mesoscutum; rounded posteriorly. Posterior margin of metanotum

extending past the posterior margin of the mesoscutum. Propodeal spiracle moderately well developed, directed posterolaterally, and separated from the propodeal declivity by about three spiracle diameters. Propodeal spines stout and short (PSI 13.2–15.6), about a quarter as long as the propodeal declivity, tapering evenly from the base and blunt. Propodeal declivity weakly concave, rounding evenly into the base of the propodeal spines. Propodeal lobes rounded and very weakly developed. Metapleural gland bulla large, extending from the metacoxal insertion three quarters of the way to the propodeal spiracle. Petiole moderately long (PLI 176–185), with flanges anterodorsally. Subpetiolar process in the form of a small, acute, triangular tooth, which grades evenly into the ventral margin of the petiole posteriorly. Petiolar peduncle short: comprising about a quarter of the total petiole length. Petiolar node erect and cuneiform: peduncle transitioning evenly into the anterior node face; anterior face forming a blunt ~90° angle with the posterior face; posterior face grading evenly into the caudal cylinder. Postpetiole evenly rounded dorsally; ventral surface weakly lobed.

In dorsal view, mesoscutum covering pronotum anteriorly, but humeri visible laterally as rounded sclerites. Propodeal spines parallel to each other, their apices separated from each other by about three times their length. Petiolar peduncle with spiracles covered by a small carina. Petiolar node, when viewed at a posterodorsal aspect, tapering dorsally; dorsal margin convex. Apex of petiolar node about a third as wide as the base; narrower than the caudal cylinder. Postpetiole narrow (PWI 128–141) and subquadrate. Anterior margin of postpetiole evenly rounding into the lateral margins, which converge slightly to the rounded posterior corners; posterior margin medially notched. Metafemur weakly incrassate (FI 234–271).

Sculpture: median clypeal carina absent, remainder with longitudinal rugulae. Lateral clypeal lobes with additional carinae; ground sculpture smooth. Antennal scapes weakly sculptured. Cephalic dorsum longitudinally rugulose, with ground sculpture weakly areolate. Fine concentric costulae surrounding the antennal insertions. Lateral surfaces of head sculptured similarly to the dorsum, but with rugulae arranged into concentric whorls around the compound eyes; rugulose sculpture between the compound eye and mandibular insertion. Ventral surface of head with weak costulae. Pronotal neck areolate. Anterior face of pronotum areolate. Lateral face of pronotum rugose anteriorly. Katepisternum, and anepisternum weakly areolate, with weak longitudinal costulae. Metapleural gland bulla with costate sculpture overlying it. Lateral face of propodeum strigulate. Propodeal declivity weakly costate. Mesoscutum and mesoscutellum with weak costulae over smooth and shining ground sculpture. Dorsum of propodeum costulate. Femora smooth and shining. Petiole predominantly areolate-rugulose. Postpetiole predominantly areolate-rugulose; anterior face smooth and shining. First gastral tergite and sternite smooth and shining, without spectral iridescence.

Setae: antennal scapes and funiculi with short, decumbent pilosity. Dorsum of the head, pronotum, waist segments, and gaster with moderately abundant, blunt setae, the longest of which are about a third of the width of the compound eye. Short, sparse pubescence present on the mesosoma.

Color: predominantly orange-yellow, with the wing bases and the posterior margin of the first gastral tergite slightly infuscated.

Male

Measurements and indices (n = 8): SL = 0.154–0.174 (0.164); FRS = 0.092–0.125 (0.115); CW = 0.545–0.568 (0.553); CWb = 0.458–0.478 (0.466); PoOC = 0.161–0.182 (0.172); CL = 0.449–0.48 (0.465); EL = 0.227–0.247 (0.235); EW = 0.195–0.212 (0.202); MD = 0.036–0.052 (0.044); WL = 0.973–1.065 (1.012); SPST = N/A; MPST = 0.197–0.244 (0.225); PEL = 0.193–0.25 (0.219); NOL = 0.153–0.182 (0.164); NOH = 0.12–0.145 (0.13); PEH = 0.167–0.19 (0.176); PPL = 0.165–0.211 (0.186); PPH = 0.172–0.196 (0.189); PW = 0.473–0.537 (0.515); SBPA = N/A; SPTI = N/A; PEW = 0.124–0.151 (0.137); PNW = 0.086–0.143 (0.119); PPW = 0.192–0.24 (0.212); HFL = 0.632–0.667 (0.647); HFWmax = 0.073–0.096 (0.087); HFWmin = 0.036–0.054 (0.047); CS = 0.456–0.478 (0.465); ES = 0.212–0.23

(0.219); SI = 33–38 (35.3); EI = 47.9–53.7 (50.5); CI = 98.9–102.9 (100.2); WLI = 212–233 (217); SBI = N/A; PSI = N/A; PWI = 144–166 (154); PLI = 103–136 (118); NI = 109–148 (128); PNWI = 68.7–113.5 (87.1); NLI = 68.6–80.3 (75.1); FI = 154–218 (188); FRSI = 19.9–26.8 (24.7); SPTII = N/A.

In full face view, head globular (CI 98.9–102.9). Mandibles very weakly striate but shining and armed with five teeth: the apical-most well developed, followed by a less developed preapical tooth and three equally developed smaller teeth. Anterior clypeal margin flat medially. Frontal carinae short, extending past the antennal toruli by about two times the maximum width of the antennal scape. Antennal scapes short: when fully retracted, failing to reach the posterior margin of the head capsule by about four times the maximum width of the scape (SI 33–38). Antennae 12-segmented; antennal club composed of four segments, with the apical-most segment about as long as the preceding two in combination. Compound eyes large and protruding past the lateral margins of the head capsule. Lateral margins of head evenly convex behind the compound eyes, rounding evenly into the posterior margin, then parallel to each other from the mandibular insertions to below the compound eyes. Posterior head margin convex, rounding evenly into the lateral margins.

In profile view, compound eyes ovular and very large (EI 47.9–53.7), with 18 ommatidia in longest row. Mesoscutum rounded evenly anteriorly, covering the dorsal surface of the pronotum, and weakly convex dorsally. Mesoscutellum on the same plain as the mesoscutum; evenly convex. Posterior margin of metanotum extending past the posterior margin of the mesoscutum. Propodeal spiracle moderately well developed, directed posterolaterally, and separated from the propodeal declivity by about three spiracle

Fig. 4. Castes of *Temnothorax caryaluteus* sp. nov. **a**–**c**. Holotype ☿ (USNM, CASENT4011115). **a**. Full face view. **b**. Profile view. **c**. Dorsal view. **d–f**. Paratype ♀ (USNM, CASENT4011128). **d**. Full face view. **e**. Profile view. **f**. Dorsal view. **g**–**i**. Non-type ♂ (USNM, CASENT4012896). **g**. Full face view. **h**. Profile view. **i**. Dorsal view. Scale bars 0.2 mm.

diameters. Propodeal spines absent, represented by blunt angles. Propodeal declivity weakly concave. Propodeal lobes rounded and very weakly developed. Petiole short (PLI 103–136), with blunt angles anterodorsally. Subpetiolar process in the form of a very small triangular tooth, which grades evenly into the ventral margin of the petiole posteriorly. Petiolar peduncle short: comprising about a one sixth of the total petiole length. Petiolar node low and evenly rounded: peduncle transitioning evenly into the anterior node face; anterior face rounding evenly into the posterior face; posterior face grading evenly into the caudal cylinder. Postpetiole evenly rounded dorsally; ventral surface weakly lobed.

In dorsal view, mesoscutum covering pronotum anteriorly, but humeri visible laterally as rounded sclerites. Petiolar node, when viewed at a posterodorsal aspect, tapering dorsally; dorsal margin convex. Apex of petiolar node about half as wide as the base; narrower than the caudal cylinder. Postpetiole narrow (PWI 144–166) and subquadrate; slightly broader anteriorly. Anterior margin of postpetiole evenly rounding into the lateral margins, which converge slightly to the rounded posterior corners; posterior margin medially notched. Metafemur thin (FI 154–218).

Sculpture: median clypeal carina absent, remainder with faint longitudinal rugulae. Lateral clypeal lobes with weakly rugulose; ground sculpture smooth. Antennal scapes smooth. Cephalic dorsum longitudinally rugulose, with ground sculpture weakly areolate. Lateral surfaces of head sculptured similarly to the dorsum, but with rugulae arranged into concentric whorls around the compound eyes; rugulose sculpture between the compound eye and mandibular insertion. Ventral surface of head weakly rugulose. Pronotal neck weakly areolate. Anterior face of pronotum weakly areolate, mostly smooth. Lateral face of pronotum smooth anteriorly. Katepisternum and anepisternum smooth and shining. Lateral face of propodeum weakly strigulate. Propodeal declivity areolate. Mesoscutum and mesoscutellum smooth and shining. Dorsum of propodeum weakly costulate. Femora smooth and shining. Petiole weakly areolate. Postpetiole predominantly smooth and shining, weakly rugulose on posterior margin. First gastral tergite and sternite smooth and shining, without spectral iridescence.

Setae: antennal scapes and funiculi with short, decumbent pilosity. Dorsum of the head, pronotum, waist segments, and gaster with moderately abundant, tapering setae, the longest of which are about a third of the width of the compound eye.

Color: predominantly pale yellow, with the head capsule, mesoscutellum, and the posterior margin of the first gastral tergite infuscated.

Distribution and ecology

Temnothorax caryaluteus sp. nov. is broadly distributed throughout the eastern United States, but apparently commonly misidentified as *T. ambiguus*, most likely due to the short propodeal spines. The geographic range of *T. caryaluteus* is contained completely within the range of *T. curvispinosus*, its closest relative (Prebus in prep.), but appears to be confined to slightly lower latitudes (see Fig. 5). We were unable to find a range overlap between *T. caryaluteus* and *T. ambiguus*, although they come into close contact in Virginia and West Virginia. It is likely that in this region their ranges are stratified by elevation, with *T. ambiguus* inhabiting mountain tops. All nest collections of *T. caryaluteus* have been taken from dead wood on live trees. The known host trees are *Carya illinoiensis* (Wangenh.) K.Koch and *Quercus montana* Willd., both of which are common and widespread hardwoods in the eastern United States. All collections have occurred below 500 m.

Notes

Temnothorax caryaluteus sp. nov. will visit blacklights, but we have only a single date associated with an alate collection event: 10 Jun. 2018 in Madison Co., AL by Steven Wang. Like the worker, the gyne of *T. caryaluteus* may be confused with that of *T. ambiguus* or *T. curvispinosus*. In agreement with Wesson & Wesson (1940), we found significant differences in the distributions of Weber's length (WL)

and pronotum width (PW) in gynes (Supp. file 3), but we hesitate to use these as diagnostic characters due to the presence of microgynes in *T. curvispinosus* in at least some parts of its range (Prebus pers. obs.). *Temnothorax caryaluteus* exhibits some integument color variation across its range. Most worker specimens that we have examined are predominantly orange-yellow, with the posterior margin of the first gastral tergite slightly infuscated, but one specimen from the vicinity of Athens, GA is predominantly medium brown (CASENT0750495).

All collections of *Temnothorax caryaluteus* sp. nov. to date have been made from under bark or in dead branches and twigs on live trees in the genera *Quercus* and *Carya*. This nesting preference is only shared by one other species of *Temnothorax* in the eastern United States: *T. schaumii*. Notably *T. curvispinosus*, a close relative of *T. caryaluteus*, is only rarely found under bark on live trees or in galls, and *T. ambiguus* has never been recorded from arboreal microhabitats (Table 1). Below, we include a reformulated and updated key to the workers of *Temnothorax* species from the eastern United States.

Synopsis of Temnothorax species of the eastern United States:

Temnothorax allardycei (Mann, 1920)
Temnothorax ambiguus (Emery, 1895)
Temnothorax americanus (Emery, 1895)
Temnothorax bradleyi (Wheeler, 1913)
Temnothorax caryaluteus sp. nov.
Temnothorax curvispinosus (Mayr, 1866)
Temnothorax duloticus (Wesson, 1937)
Temnothorax longispinosus (Roger, 1863)
Temnothorax minutissimus (Smith, 1942)

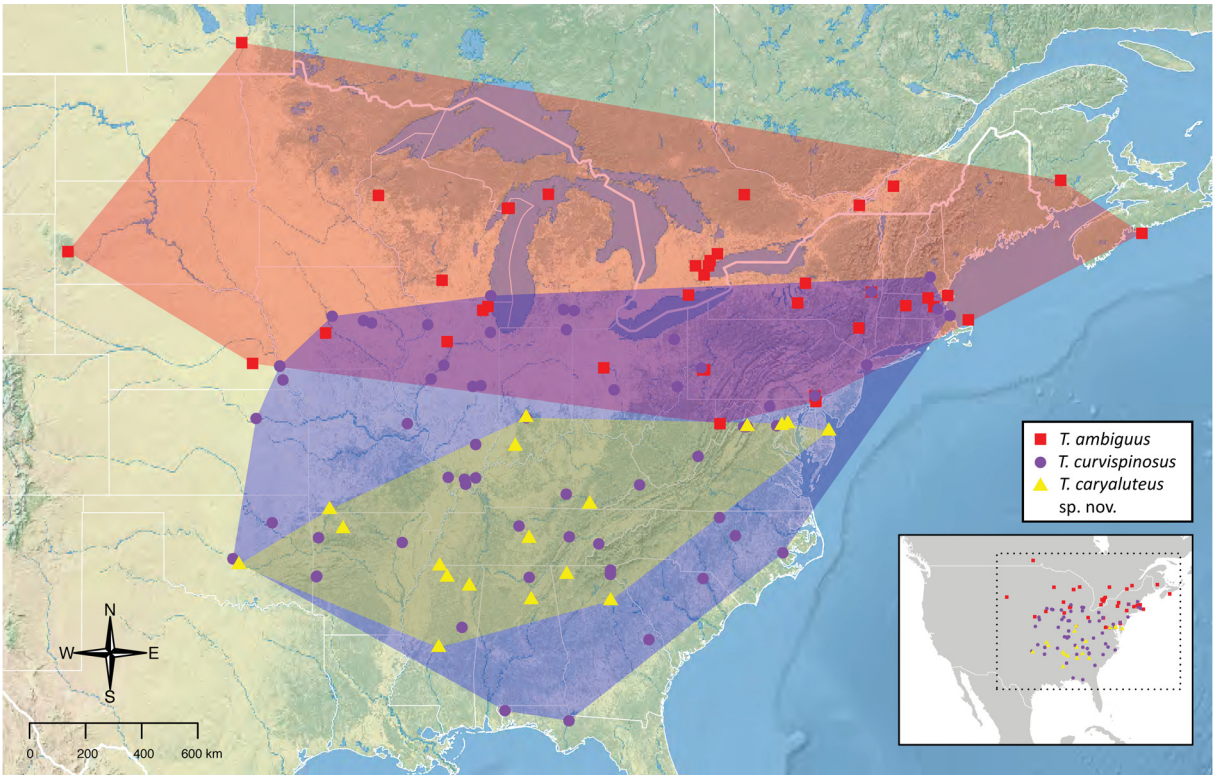

Fig. 5. Distribution map comparing the ranges of *Temnothorax caryaluteus* sp. nov., *T. ambiguus* (Emery, 1895), and *T. curvispinosus* (Mayr, 1866) in North America.

Table 1. Comparison of nesting microhabitats of species of *Temnothorax* Mayr, 1861 from the eastern United States.

	nest microhabitat											
***Temnothorax* sp.**	**Acorns / hickory nuts**	**Sticks / dead roots in leaf litter**	**Rotten logs / dead standing trees**	**Hollow plant stems**	**Rock crevices**	***Formica* nests**	**Nests of other *Temnothorax* spp.**	**Under rock/ directly in soil**	**Galls**	**Under bark on live trees**	**Hollow twigs on live trees**	**Branches on live trees**
T. allardycei (Mann, 1920)	–	x	–	x	–	–	–	–	–	–	x	–
T. ambiguus (Emery, 1895)	x	x	–	x	–	x	–	x	–	–	–	–
T. americanus (Emery, 1895)	x	x	–	–	–	–	x	–	–	–	–	–
T. bradleyi (Wheeler, 1913)	–	–	–	–	–	–	–	–	–	x	–	–
T. caryaluteus sp. nov.	–	–	–	–	–	–	–	–	–	x	x	x
T. curvispinosus (Mayr, 1866)	x	x	x	x	–	–	–	x	x	x	–	–
T. duloticus (Wesson, 1937)	x	x	–	–	–	–	x	–	–	–	–	–
T. longispinosus (Roger, 1863)	x	x	x	–	x	–	–	x	–	–	–	–
T. minutissimus (Smith, 1942)	x	–	–	–	–	–	x	–	–	–	–	–
T. palustris (Cover & Deyrup, 2004)	–	–	–	–	–	–	–	x	–	–	–	–
T. pergandei (Emery, 1895)	x	x	x	x	x	–	–	x	–	–	–	–
T. pilagens Seifert *et al.*, 2014	x	x	–	–	–	–	x	–	–	–	–	–
T. schaumii (Roger, 1863)	–	–	x	–	–	–	–	–	x	x	x	x
T. smithi (Baroni Urbani, 1978)	–	–	x	–	–	–	–	–	–	x	–	–
T. texanus (Wheeler, 1903)	–	–	–	–	–	–	–	x	–	–	–	–
T. torrei (Aguayo, 1931)	–	x	–	–	–	–	–	–	–	–	–	–
T. tuscaloosae (Wilson, 1951)	x	x	–	–	–	–	–	x	–	–	–	–

Temnothorax palustris (Cover & Deyrup, 2004)
Temnothorax pergandei (Emery, 1895)
Temnothorax pilagens Seifert *et al.*, 2014
Temnothorax schaumii (Roger, 1863)
Temnothorax smithi (Baroni Urbani, 1978)
Temnothorax texanus (Wheeler, 1903)
Temnothorax torrei (Aguayo, 1931)
Temnothorax tuscaloosae (Wilson, 1951)

Key to Temnothorax species of the eastern United States based on the worker caste

1. Antennae with 11 segments 2
– Antennae with 12 segments 13

2. Antennal scrobe present; mandible with 3-4 teeth (see Fig. 6a); dulotic social parasite of *T. ambiguus*, *T. curvispinosus* and *T. longispinosus*; widespread: Quebec, Canada south to Georgia, west to Kansas ..... ***T. americanus*** (Emery, 1895)
– Antennal scrobe absent; mandible variable, but usually with 5 teeth (see Fig. 6b); social parasite or free-living 3

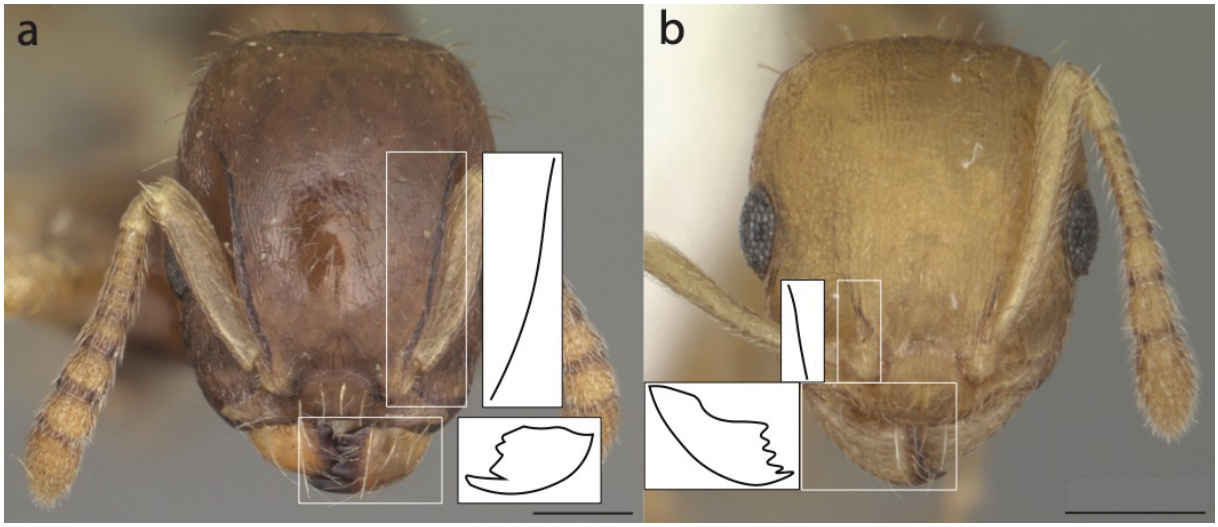

Fig. 6. Comparison of antennal scrobe and mandibular dentition characters in full face view. **a**. *Temnothorax americanus* (Emery, 1895) (☿, CASC, CASENT0104553). **b**. *T. curvispinosus* (Mayr, 1866) (☿, ABS, CASENT0104032). Photographs by April Nobile. Scale bars 0.2 mm.

3. Only apical and preapical masticatory teeth developed and acute, remainder of masticatory teeth reduced to shallow crenulae (see Fig. 7a)..... 4
– Masticatory teeth well developed, with 5 acute teeth (see Fig. 7b)..... 5

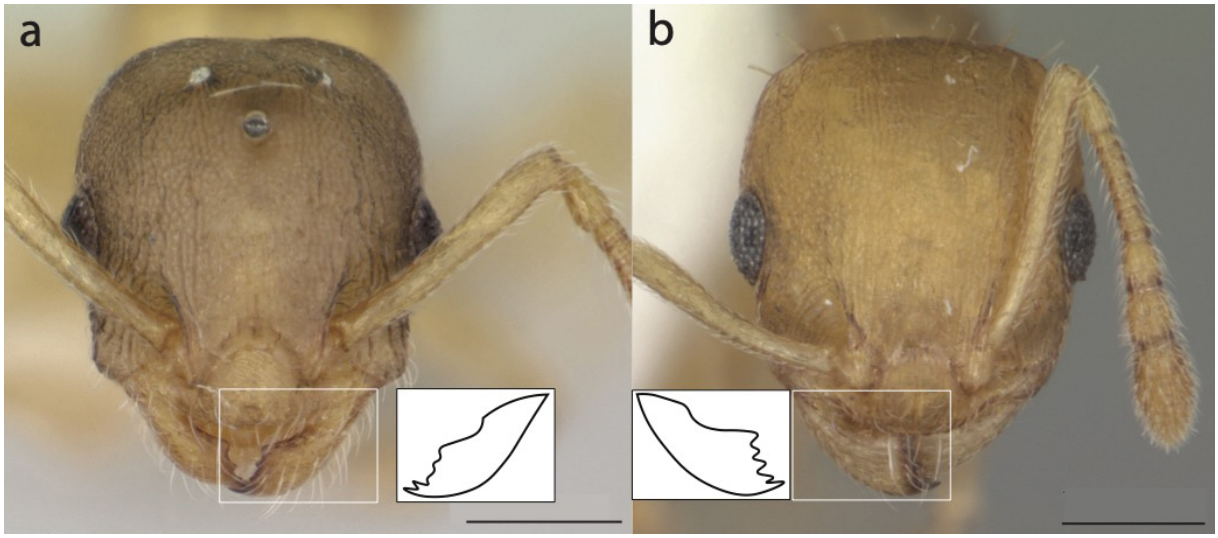

Fig. 7. Comparison of mandibular dentition characters in full face view **a**. *Temnothorax minutissimus* (Smith, 1942) (♀, LACM, CASENT0172598). **b**. *T. curvispinosus* (Mayr, 1866) (☿, ABS, CASENT0104032). Photographs by April Nobile. Scale bars 0.2 mm.

4. Only known from the sexual castes; queen minute: ~ 3 mm in length (Fig. 8a); obligate inquiline social parasite of *T. curvispinosus*; rare: New York south to North Carolina, west to Indiana and Michigan..... ***T. minutissimus*** (M.R. Smith, 1942)
– Worker and sexual castes present (Fig. 8b); queen larger: > 3 mm in length; dulotic social parasite of *T. ambiguus* and *T. longispinosus*; rare: Vermont, west to Ontario and Michigan..... ***T. pilagens*** Seifert *et al.*, 2014

Fig. 8. Comparison of *Temnothorax minutissimus* (Smith, 1942) and *T. pilagens* Seifert *et al.*, 2014 in profile view. **a**. *Temnothorax minutissimus* (♀, LACM, CASENT0172598; photograph by April Nobile). **b**. *T. pilagens* (☿, MMPC, CASENT0868793; photograph by Matthew Prebus). Scale bars 0.2 mm.

5. Antennal scapes short, failing to reach the posterior margin of the head by ≥ 2 antennal scape widths when fully retracted (see Fig. 9a–c); arboreal species nesting in dead branches on live trees, in tree cavities, or under bark.....6 (***rugatulus*** clade sensu Prebus 2021)
– Antennal scapes long: if failing to reach the posterior margin of the head when fully retracted, then they do so by < 2 (usually < 1) antennal scape widths (see Fig. 9d–f); arboreal or not .....8 (***longispinosus*** group)

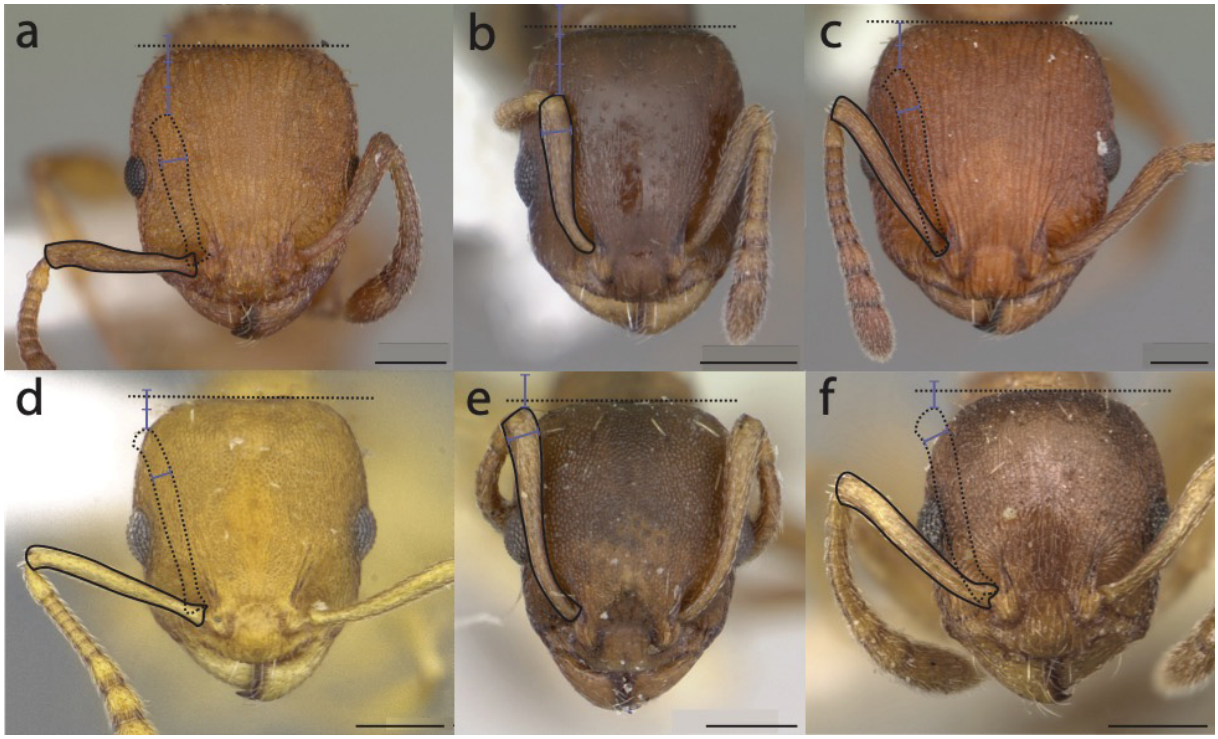

Fig. 9. Comparison of antennal scape lengths in full face view. **a**. *Temnothorax bradleyi* (Wheeler, 1913) (☿, ABS, CASENT0104011; photograph by April Nobile). **b**. *T. schaumii* (Roger, 1863) (☿, ABS, CASENT0104047; photograph by April Nobile). **c**. *T. smithi* (Baroni Urbani, 1978) (☿, ABS, CASENT0104053; photograph by April Nobile). **d**. *T. caryaluteus* sp. nov. (holotype ☿, USNM, CASENT4011115; photograph by Matthew Prebus). **e**. *T. duloticus* (Wesson, 1937) (☿, USNM, CASENT0103163; photograph by April Nobile). **f**. *T. ambiguus* (Emery, 1895) (☿, MSNG, CASENT0904763; photograph by Will Ericson). Scale bars 0.2 mm.

6. Propodeal spines long: about as long as the propodeal declivity in profile view (see Fig. 10a); nests in cavities under bark; widespread: Ohio south to Florida, west to Mississippi and Indiana ..... ***T. smithi*** (Baroni Urbani, 1978)
– Propodeal spines short: shorter than the propodeal declivity in profile view (see Fig. 10b–c); widespread; nesting under bark or in branches..... 7

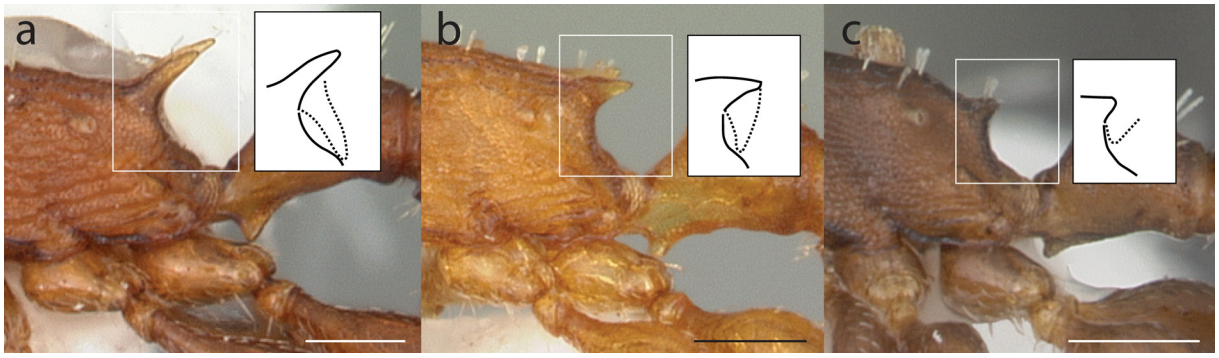

Fig. 10. Comparison of *Temnothorax* propodeal spines in profile view; inset drawings depict propodeal spine length (dotted outlines) in comparison to length of the propodeal declivity. **a**. *Temnothorax bradleyi* (Wheeler, 1913) (☿, ABS, CASENT0104011). **b**. *T. smithi* (Baroni Urbani, 1978) (☿, ABS, CASENT0104053). **c**. *T. schaumii* (Roger, 1863) (☿, ABS, CASENT0104047). Photographs by April Nobile, from www.antweb.org. Scale bars 0.2 mm.

7. Head densely sculptured in full face view: covered in longitudinal rugae, with the interstices densely areolate (see Fig. 11a); nests in hollow cavities under bark; North Carolina south to Florida, west to Louisiana and Tennessee ..... ***T. bradleyi*** (W.M. Wheeler, 1913)
– Head less sculptured in full face view: mostly smooth and shining, with weak longitudinal rugulae and weak areolae around the compound eyes and radiating posteriorly from the antennal insertions (see Fig. 11b); nests in upper branches of mature oaks and hickories; widespread: Maine south to Florida, west to New Mexico and Nebraska..... ***T. schaumii*** (Roger, 1863)

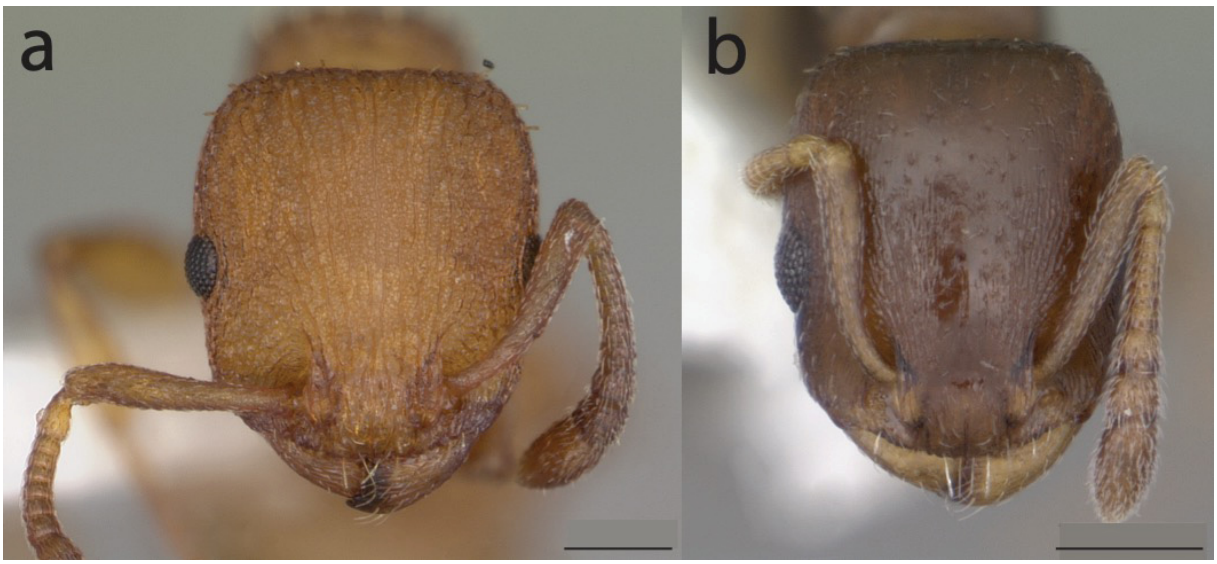

Fig. 11. Comparison of head integument sculpture in full face view. **a**. *Temnothorax bradleyi* (Wheeler, 1913) (☿, ABS, CASENT0104011). **b**. *T. schaumii* (Roger, 1863) (☿, ABS, CASENT0104047). Photographs by April Nobile, from www.antweb.org. Scale bars 0.2 mm.

8. Subpostpetiolar process present and enlarged (see Fig. 12a); dulotic social parasite of *T. ambiguus*, *T. curvispinosus*, and *T. longispinosus*; New York south to Georgia, west to Illinois ..... ***T. duloticus*** (L.G. Wesson, 1937)
– Subpostpetiolar process absent or weakly developed (see Fig. 12b–c); free living species..... 9

Fig. 12. Comparison of subpostpetiolar processes in profile view. **a**. *Temnothorax duloticus* (Wesson, 1937) (☿, SMNG, ANTWEB1008479; photograph by Roland Schultz). **b**. *T. ambiguus* (Emery, 1895) (☿, UCDC, CASENT0104803; photograph by April Nobile). **c**. *T. longispinosus* (Roger, 1863) (☿, USNM, CASENT0105559; photograph by Dan Kjar). Scale bars 0.2 mm.

9. Propodeal spines shorter than, or as long as, the propodeal declivity in profile view (see Fig. 13a–b) 10
– Propodeal spines much longer than the propodeal declivity in profile view (see Fig. 13c–d) 12

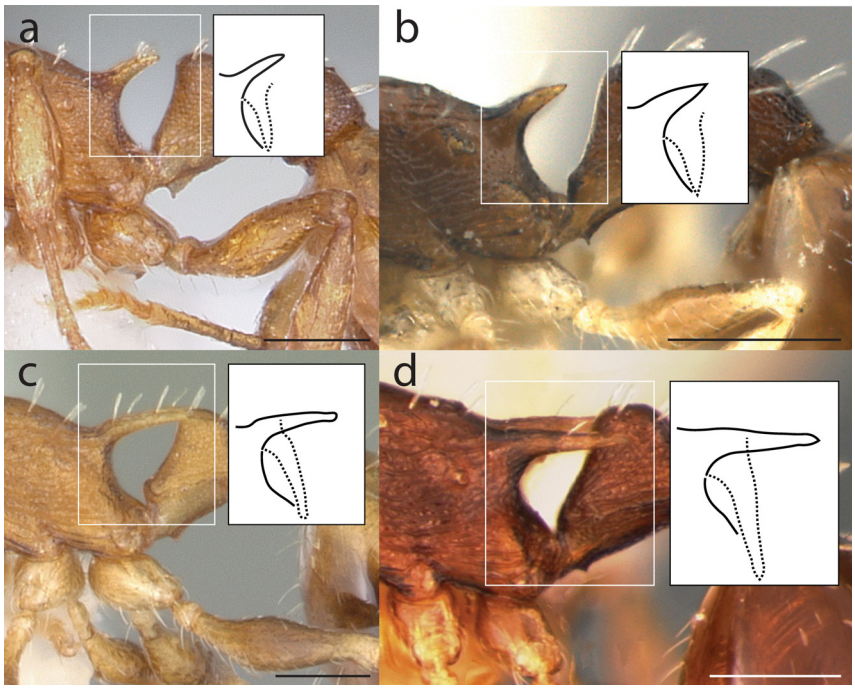

Fig. 13. Comparison of *Temnothorax* propodeal spines in profile view; inset drawings depict propodeal spine length (dotted outlines) in comparison to length of the propodeal declivity **a**. *T. ambiguus* (Emery, 1895) (☿, UCDC, CASENT0104803; photograph by April Nobile). **b**. *T. tuscaloosae* (Wilson, 1951) (syntype ☿, MCZC; photograph by Gary Alpert). **c**. *T. curvispinosus* (Mayr, 1866) (☿, ABS, CASENT0104040; photograph by April Nobile). **d**. *T. longispinosus* (Roger, 1863) (☿, USNM, CASENT0105559; photograph by Dan Kjar). Scale bars 0.2 mm.

10. Dorsum of mesosoma mostly smooth and shining (see Fig. 14a); workers small: ~ 2 mm in length; head, mesosoma, and gaster with dark integument; nests in small cavities in soil, hickory nuts, or acorns; Virginia south to Florida, west to Mississippi and Tennessee..... ***T. tuscaloosae*** (Wilson, 1951)
– Dorsum of mesosoma sculptured (see Fig. 14b); workers larger: > 3 mm in length; head, mesosoma, and gaster with light colored integument.....11

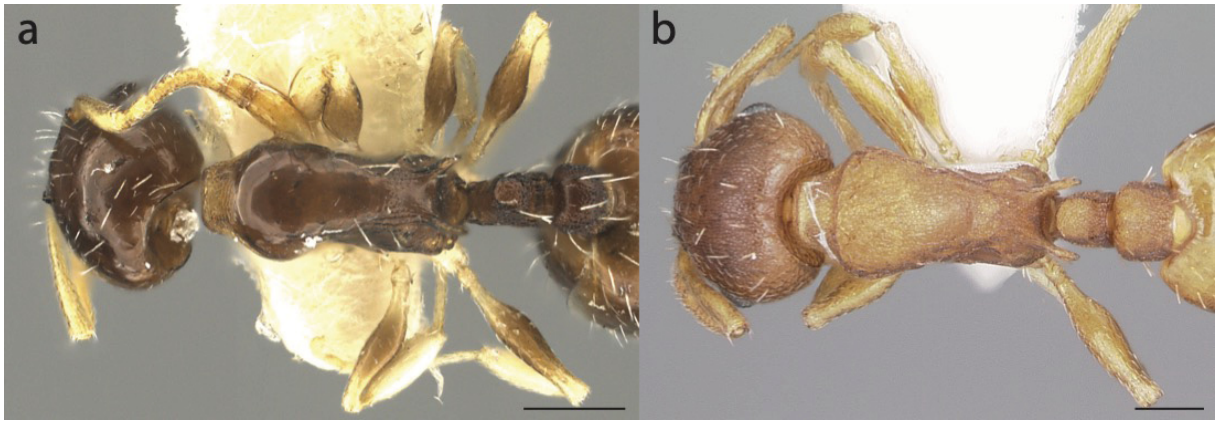

Fig. 14. Comparison of mesosoma integument sculpture in dorsal view. **a**. *Temnothorax tuscaloosae* (Wilson, 1951) (syntype ☿, MCZC; photograph by Gary Alpert). **b**. *T. ambiguus* (Emery, 1895) (☿, UCDC, CASENT0104803; photograph by April Nobile). Scale bars 0.2 mm.

11. Propodeal spines closely approximated at base, their union forming a U-shape with a narrow base (see Fig. 15a); petiolar node acute to narrowly rounded in profile view, narrower than petiole in dorsal view (see Fig.15a); mesosoma slightly arched in profile view (see Fig. 15b); nests in hollow twigs, in branches, and under bark on live trees; widespread: Delaware south to Mississippi, west to Oklahoma (see Fig. 5)..... ***T. caryaluteus*** sp. nov.
– Propodeal spines further apart at base, their union forming a squared-off, broad-based U-shape (see Fig. 15c); petiolar node broadly rounded or with a distinct dorsal face in profile view, about as broad as petiole in dorsal view (see Fig. 15c); mesosoma flat in profile view (see Fig. 15d); nests in hollow acorns, hickory nuts, and hollow twigs in the leaf litter; widespread: Nova Scotia south to West Virginia, west to South Dakota and Manitoba (see Fig. 4)..... ***T. ambiguus*** (Emery, 1895)

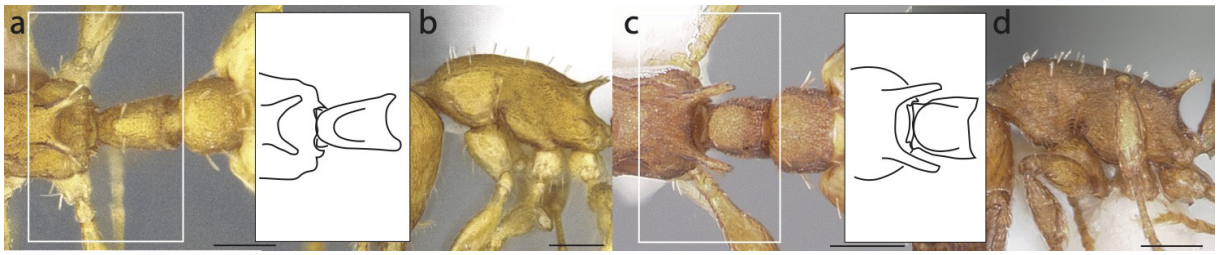

Fig. 15. Comparison of propodeal spine and mesosoma profile characters. **a**–**b**. *Temnothorax caryaluteus* sp. nov. (holotype ☿, USNM, CASENT4011115, photographs by Matthew Prebus). **a**. Dorsal view. **b**. Profile view. **c**–**d**. *T. ambiguus* (Emery, 1895) (☿, UCDC, CASENT0104803, photographs by April Nobile). **c**. Dorsal view. **d**. Profile view. Scale bars 0.2 mm.

12. Integument typically light colored; head densely sculptured (see Fig. 16a); propodeal spines bent in profile view (see Fig. 16b); nests in hollow acorns, hickory nuts, and hollow twigs in the leaf litter; widespread: New Hampshire south to Florida, west to Oklahoma and Iowa (see Fig. 5)..... ***T. curvispinosus*** (Mayr, 1866)
– Integument typically dark colored; head sculpture variable, ranging from mostly smooth to densely sculptured (see Fig. 16c); propodeal spines straight in profile view (see Fig. 16d); nests in hollow acorns, hickory nuts, and hollow twigs in the leaf litter; widespread: Quebec, Canada south to Georgia, west to Arkansas and Minnesota..... ***T. longispinosus*** (Roger, 1863)

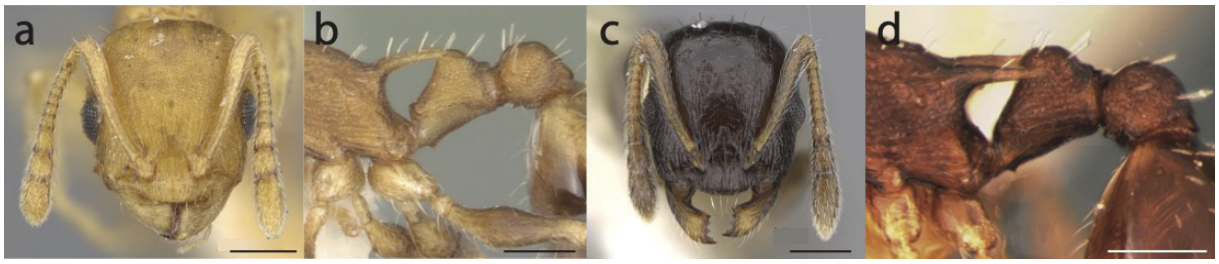

Fig. 16. Comparison of head integument sculpture and propodeal spine characters. **a**–**b**. *Temnothorax curvispinosus* (Mayr, 1866). **a**. Full face view (☿, NHMUK, CASENT0901789; photograph by Will Ericson). **b**. Profile view (☿, ABS, CASENT0104040; photograph by April Nobile). **c**–**d**. *T. longispinosus* (Roger, 1863). **c**. Full face view (☿, CASC, CASENT0914508; photograph by Dominique Monie). **d**. Profile view (☿, USNM, CASENT0105559; photograph by Dan Kjar). Scale bars 0.2 mm.

13. Metanotal groove deeply impressed (see Fig. 17a); nests in stumps, logs, nutshells, or in the soil; widespread: New Jersey south to Hidalgo, Mexico, west to Arizona and Nebraska..... ..... ***T. pergandei*** (Emery, 1895)
– Metanotal groove not deeply impressed (see Fig. 17b–c) 14

14. Mesosoma arched (see Fig. 17b) 15
– mesosoma not arched (see Fig. 17c)..... 16

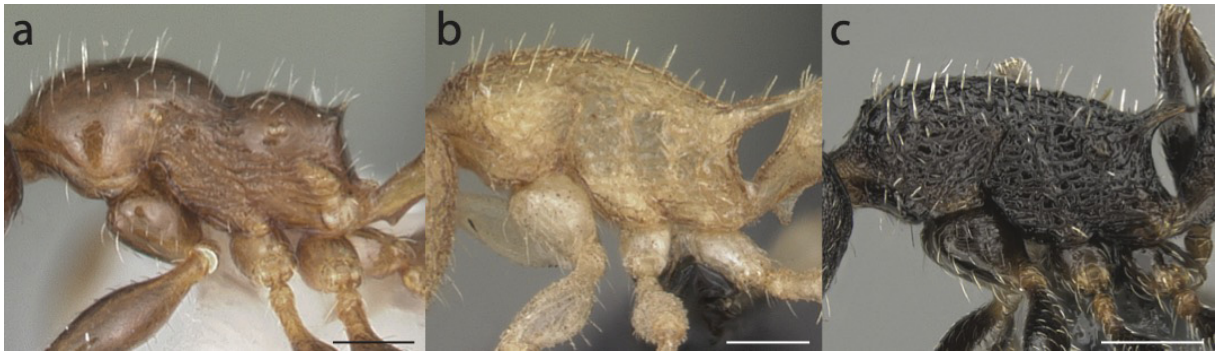

Fig. 17. Comparison of mesosoma profile characters in profile view. **a**. *Temnothorax pergandei* (Emery, 1895) (☿, ABS, CASENT0104016; photograph by April Nobile). **b**. *T. allardycei* (Mann, 1920) (☿, ABS, CASENT0104009; photograph by April Nobile). **c**. *T. texanus* (Wheeler, 1903) (☿, CASC, CASENT0923379; photograph by Michele Esposito). Scale bars 0.2 mm.

15. Dorsum of petiole with two setae (see Fig. 18a); head lightly sculptured (see Fig. 18b); nesting in leaf litter; southern Florida and the Caribbean ..... ***T. torrei*** (Aguayo, 1931)
– Dorsum of petiole with > 2 setae (see Fig. 18c); head densely sculptured (see Fig. 18d); nesting in hollow twigs, vines, and culms of sawgrass; southern Florida and the Caribbean ..... ***T. allardycei*** (Mann, 1920)

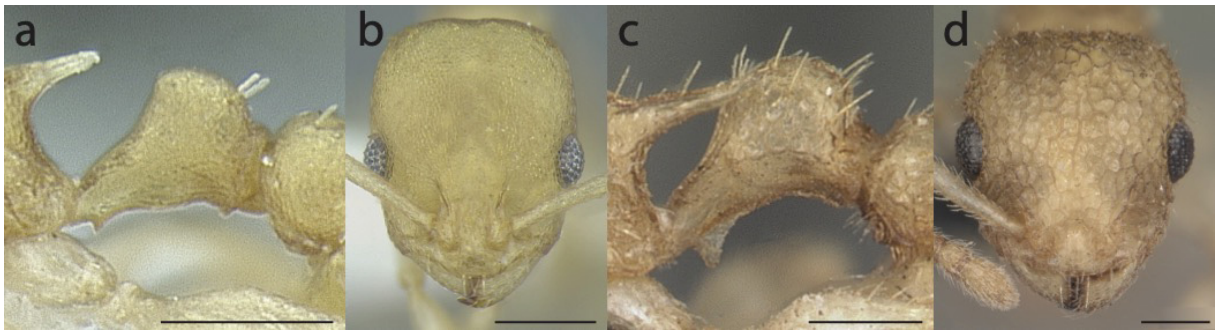

Fig. 18. Comparison of propodeal node setae and head integument sculpture. **a**–**b**. *Temnothorax torrei* (Aguayo, 1931) (☿, MCZC, MCZENT00583611, photograph by Matthew Prebus). **a**. Profile view. **b**. Full face view. **c**–**d**. *T. allardycei* (Mann, 1920) (☿, ABS, CASENT0104009; photograph by April Nobile). **c**. Profile view. **d**. Full face view. Scale bars 0.2 mm.

16. Integument typically dark colored; postpetiole wider than long in dorsal view (see Fig. 19a); ground nesting; occurring in open to semi-open sites with well-drained soil; widespread: Massachusetts south to Florida, west to New Mexico and Minnesota ..... ***T. texanus*** (W.M. Wheeler, 1903)
– Integument typically light colored; postpetiole about as wide as long in dorsal view (see Fig. 19b); ground nesting; occurs in marshes of the Florida panhandle .... ***T. palustris*** (Cover & Deyrup, 2004)

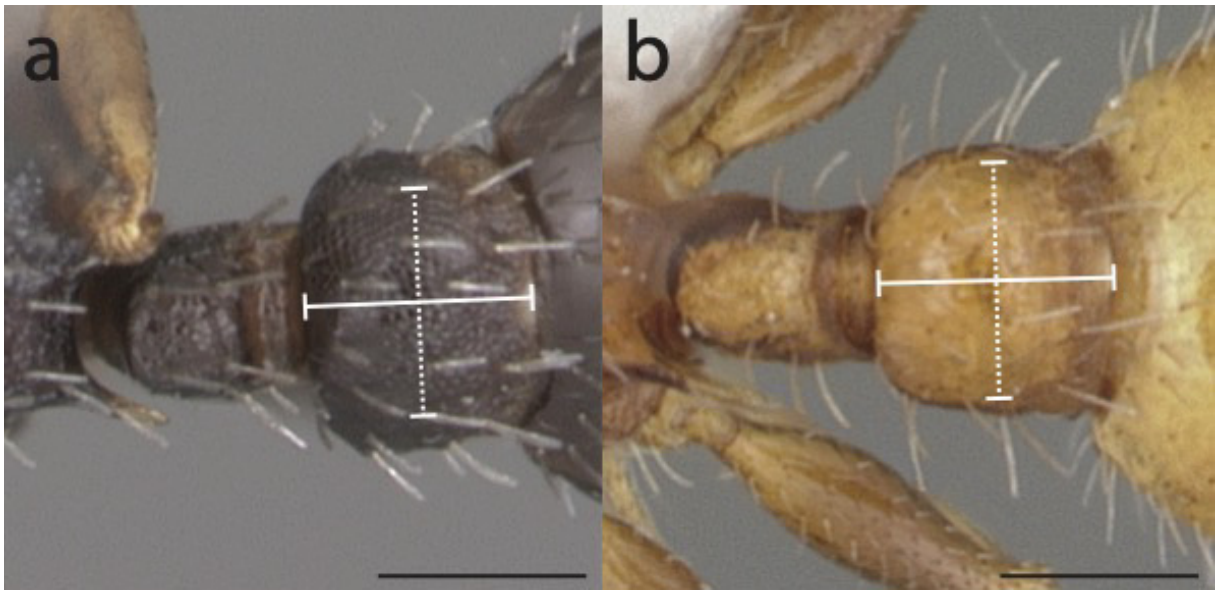

Fig. 19. Comparison of postpetiole proportions in dorsal view. **a**. *Temnothorax texanus* (Wheeler, 1903) (☿, ABS, CASENT0104063). **b**. *T. palustris* (Cover & Deyrup, 2004) (☿, ABS, CASENT0104045). Photographs by April Nobile. Scale bars 0.2 mm.

Discussion

It is almost certain that this species has been represented in the literature previously: Wesson & Wesson (1940) discussed what they interpreted as a variety of *T. curvispinosus*, based on nest collections from dead twigs and cavities in the bark of living or recently fallen oak trees. The following is an excerpt from Wesson & Wesson (1940: 96–97): "The workers differ from the worker of the typical curvispinosus in (1) the short epinotal spines which vary from as long as broad to twice as long as broad at the base; (2) the less convex posterior slope of the petiole; (3) the more uniform rugosity on the sides and dorsum of the thorax; (4) the average paler, smaller and more diffuse dark spots on the gaster. The female, which also seems to be distinct, differs from the female of typical curvispinosus in (1) the very short epinotal spines which are shorter than broad at the base; (2) the somewhat less robust thorax; (3) the paler and less extensive infuscation, particularly on the gaster. In view of the variability of curvispinosus, we hesitate to describe this tree-living formula as a distinct variety until we have been able to examine much more material. Winged phases were taken in early July."

Unfortunately, we have not been able to locate the collections associated with the above article, and so are unable to verify whether these are *T. caryaluteus* sp. nov.

Temnothorax is a hyperdiverse genus of myrmicine ants that is broadly distributed throughout the northern hemisphere. Due to its small nest sizes and tolerance for lab conditions, a handful of *Temnothorax* species have been used extensively in behavioral and physiological experiments, which has contributed to *Temnothorax curvispinosus* being among the most thoroughly studied of ant species. Despite this attention, and the hundreds of named *Temnothorax* species globally, new species of this genus are still being described at a rapid pace, especially from the American tropics and Eastern Asia. The eastern United States, however, has received a large amount of attention from taxonomists, ecologists, and citizen scientists alike. Considering this, finding new species in this region is a rare event. Our results clarify key characteristics that distinguish *Temnothorax caryaluteus* sp. nov. from *T. curvispinosus*, a close relative which it closely resembles morphologically (and which it significantly overlaps with geographically), and *T. ambiguus*, which *T. caryaluteus* has been systematically mistaken for in collections.

The eastern North American dulotic social parasite *T. americanus* and the closely related *T. longispinosus* species group (composed of *T. ambiguus*, *T. caryaluteus* sp. nov., *T. curvispinosus*, *T. duloticus*, *T. longispinosus*, *T. minutissimus*, *T. pilagens*, and *T. tuscaloosae*), are well known for their importance as subjects in the study of ant social parasitism. Of the eight species currently recognized in the *T. longispinosus* group, three are socially parasitic (*T. duloticus*, *T. minutissimus*, and *T. pilagens*), and three are hosts to social parasites (*T. ambiguus*, *T. curvispinosus*, and *T. longispinosus*). Notably, these three host species have workers that are more-or-less average sized for *Temnothorax* (average WL for *T. ambiguus* and *T. curvispinosus* is 0.7 mm for both species in this study) and are predominantly terrestrially nesting, often in rotten tree nut shells and dead sticks in the leaf litter. The two non-host *longispinosus* group species diverge morphologically and ecologically from these host species: *T. tuscaloosae* is generally smaller (WL reported as 0.554 mm by Wilson 1951), and *T. caryaluteus* is arboreally nesting. These traits may represent two adaptations in response to selective pressures imposed by social parasites, with *T. tuscaloosae* workers providing insufficient nutrition for social parasite brood development, and with *T. caryaluteus* becoming undetectable to social parasites adapted to finding terrestrial hosts. However, more study is required to support these claims.

In this study, we were able to extend our initial distribution map of *Temnothorax caryaluteus* sp. nov. and update our understanding of the distribution of *T. ambiguus* with the help of photographs taken by amateur naturalists. As a result, *T. ambiguus* was found to have a more northerly distribution than is currently represented in distribution maps, highlighting the need for re-evaluation of this species in collections. Along with the updated key to *Temnothorax* of the eastern United States, these results provide an important resource for professionals, citizen scientists, and amateur naturalists alike.

Data availability

Raw morphometric data and the R scripts used for analyses in this study are available on Dryad: https://doi.org/10.5061/dryad.tb2rbp08q; Prebus *et al.* (2024).

Funding

This project was supported by the US National Science Foundation (NSF CAREER DEB-1943626), the Social Insect Research Group (SIRG) at Arizona State University, the University of Hohenheim, and the Carl-Zeiss-Foundation.

Acknowledgments

Thank you to Brendon Boudinot, Mark Deyrup, Chris Grinter, Benoit Guenard, Rick Hoebeke, Ken Howard, Kal Ivanov, Petr Klimes, Jack Longino, Joe MacGown, Nolan Novotny, Joe Ruhe, Phil Ward, and Alex Wild for loans and donations of specimens. Additional thanks go to Earl Agpawa, James Bailey, Eric Blomberg, Jean Brodeur, Benjamin Burgunder, Ben Coulter, Jeffrey G. Cramer, Robby Deans, Charley Eiseman, Solomon Hendrix, Michael H. King, Antonio Liberta, Ilona Loser, Stephen Luk, Chase G. Mayers, Max McCarthy, Ramóna Molnár, Tom Murray, Martha O'Kennon, Séraphin Poudrier, Bryan E. Reynolds, Jesse Rorabaugh, John Rosenfeld, Katja Schulz, Thomas Shahan, Ryan Sorrells, A.W. Thomas, Kari Thompson, Daniel Ulrich, Steven Wang, chipperatl, and anglersent for allowing us to use their observation data for this study. Sarah Farmer, Kalen Breland, Jessica Nickelsen, Teresa Jackson, Jacqueline Patterson, and Bradi McDonald of the United States Forest Service helped organize and coordinate the school outreach project and social media campaign. Special thanks to Didi Miller-Anders, Alex Ruiz, Antonio Motola, Benjamin Pauly, Brodie Gaudie, Sara Clarke, Clay Birchfield, Giovanni Tallino, Jay Avery, Jcactus57, Kathy Hoff, Meagan Hunter, Melissa Parker, Terri O'Donnell, Pam Evans Ward, Phillip & Bekah Duncan, Rocky Montoya, and Scott Bloom for proposing names for the new species. Finally, we thank two anonymous peer reviewers for comments and corrections that substantially improved this article.

References

Achenbach A. & Foitzik S. 2009. First evidence for slave rebellion: enslaved ant workers systematically kill the brood of their social parasite *Protomognathus americanus*. *Evolution* 63: 1068–1075. https://doi.org/10.1111/j.1558-5646.2009.00591.x

Beckers R., Goss S., Deneubourg J.L. & Pasteels J.M. 1989. Colony size, communication and ant foraging strategy. *Psyche: A Journal of Entomology* 96(3–4): 239–256. https://doi.org/10.1155/1989/94279

Beibl J., Stuart R.J., Heinze J. & Foitzik S. 2005. Six origins of slavery in formicoxenine ants. *Insectes Sociaux* 52: 291–297. https://doi.org/10.1007/s00040-005-0808-y

Blatrix R. & Herbers J.M. 2004. Intracolonial conflict in the slave-making ant *Protomognathus americanus*: dominance hierarchies and individual reproductive success. *Insectes Sociaux* 51: 131–138. https://doi.org/10.1007/s00040-003-0710-4

Bolton B. 2024. An online catalog of the ants of the world. Available from https://antcat.org. [accessed 24 Jul. 2024].

Booher D., MacGown J.A., Hubbell S.P. & Duffield R.M. 2017. Density and dispersion of cavity dwelling ant species in nuts of eastern US forest floors. *Transactions of the American Entomological Society* 143: 79–93. https://doi.org/10.3157/061.143.0105

Cole B.J. 1981. Dominance hierarchies in *Leptothorax* ants. *Science* 212: 83–84. https://doi.org/10.1126/science.212.4490.83

Csősz S. & Fisher B.L. 2015. Diagnostic survey of Malagasy *Nesomyrmex* species-groups and revision of *hafahafa* group species via morphology based cluster delimitation protocol. *ZooKeys* 526: 19–59. https://doi.org/10.3897/zookeys.526.6037

Foitzik S., Backus V.L., Trindl A. & Herbers J.M. 2004. Ecology of *Leptothorax* ants: impact of food, nest sites, and social parasites. *Behavioral Ecology and Sociobiology* 55: 484–493. https://doi.org/10.1007/s00265-003-0718-9

Herbers J.M. & Johnson C.A. 2007. Social structure and winter survival in acorn ants. *Oikos* 116: 829–835. https://doi.org/10.1111/j.0030-1299.2007.15679.x

Jongepier E., Kleeberg I. & Foitzik S. 2015. The ecological success of a social parasite increases with manipulation of collective host behaviour. *Journal of Evolutionary Biology* 28: 2152–2162. https://doi.org/10.1111/jeb.12738

Kassambara A. 2023. ggpubr: 'ggplot2' Based Publication Ready Plots. R package version 0.6.0. Available from https://rpkgs.datanovia.com/ggpubr/ [accessed 22 Oct. 2024].

Linksvayer T.A. 2008. Queen–worker–brood coadaptation rather than conflict may drive colony resource allocation in the ant *Temnothorax curvispinosus*. *Behavioral Ecology and Sociobiology* 62: 647–657. https://doi.org/10.1007/s00265-007-0489-9

Möglich M., Maschwitz U. & Holldobler B. 1974. Tandem calling: a new kind of signal in ant communication. *Science* 186: 1046–1047. https://doi.org/10.1126/science.186.4168.1046

Pratt S.C. & Pierce N.E. 2001. The cavity-dwelling ant *Leptothorax curvispinosus* uses nest geometry to discriminate between potential homes. *Animal Behaviour* 62: 281–287. https://doi.org/10.1006/anbe.2001.1777

Pratt S.C., Mallon E.B., Sumpter D.J. & Franks N.R. 2002. Quorum sensing, recruitment, and collective decision-making during colony emigration by the ant *Leptothorax albipennis*. *Behavioral Ecology and Sociobiology* 52: 117–127. https://doi.org/10.1007/s00265-002-0487-x

Prebus M. 2015. Palearctic elements in the old world tropics: a taxonomic revision of the ant genus *Temnothorax* Mayr (Hymenoptera, Formicidae) for the Afrotropical biogeographical region. *ZooKeys* 483: 23–57. https://doi.org/10.3897/zookeys.483.9111

Prebus M. 2017. Insights into the evolution, biogeography and natural history of the acorn ants, genus *Temnothorax* Mayr (Hymenoptera: Formicidae). *BMC Evolutionary Biology* 17: 1–22. https://doi.org/10.1186/s12862-017-1095-8

Prebus M.M. 2021. Taxonomic revision of the *Temnothorax salvini* clade (Hymenoptera: Formicidae), with a key to the clades of New World *Temnothorax*. *PeerJ* 9: e11514. https://doi.org/10.7717/peerj.11514

Prebus M.M., Nguyen N., Doering G.N. & Booher D. 2024. Data from: *Temnothorax caryaluteus* sp. nov. (Hymenoptera: Formicidae): a new ant species from the eastern United States [Dataset]. *Dryad.* https://doi.org/10.5061/dryad.tb2rbp08q

R Core Team 2022. R: A language and environment for statistical computing. R Foundation for Statistical Computing, Vienna, Austria. Available from https://www.R-project.org/ [accessed 22 Oct. 2024].

Rüppell O., Heinze J. & Hölldobler B. 2001. Alternative reproductive tactics in the queen-size-dimorphic ant *Leptothorax rugatulus* (Emery) and their consequences for genetic population structure. *Behavioral Ecology and Sociobiology* 50: 189–197. https://doi.org/10.1007/s002650100359

Seifert B. & Csősz S. 2015. *Temnothorax crasecundus* sp. n.–a cryptic Eurocaucasian ant species (Hymenoptera, Formicidae) discovered by Nest Centroid Clustering. *ZooKeys* 479: 37–64. https://doi.org/10.3897/zookeys.479.8510

Seifert B., Kleeberg I., Feldmeyer B., Pamminger T., Jongepier E. & Foitzik S. 2014. *Temnothorax pilagens* sp. n. – a new slave-making species of the tribe Formicoxenini from North America (Hymenoptera, Formicidae). *ZooKeys* 368: 65-77. https://doi.org/10.3897/zookeys.368.6423

Stuart R.J. 1985. Spontaneous polydomy in laboratory colonies of the ant *Leptothorax curvispinosus* Mayr (Hymenoptera; Formicidae). *Psyche* 92: 71–81. https://doi.org/10.1155/1985/29215

Talbot M. 1957. Population studies of the slave-making ant *Leptothorax duloticus* and its slave, *Leptothorax curvispinosus*. *Ecology* 38: 449–456. https://doi.org/10.2307/1929889

Wesson L.G. & Wesson R.G. 1940. A collection of ants from southcentral Ohio. *American Midland Naturalist* 24: 89–103. https://doi.org/10.2307/2421055

Wilson E.O. 1951. A new *Leptothorax* from Alabama (Hymenoptera: Formicidae). *Psyche (Cambridge)* 57: 128–130. https://doi.org/10.1155/1950/35317

Wilson E.O. 1974. Aversive behavior and competition within colonies of the ant *Leptothorax curvispinosus*. *Annals of the Entomological Society of America* 67: 777–780. https://doi.org/10.1093/aesa/67.5.777

Manuscript received: 29 March 2024
Manuscript accepted: 1 August 2024
Published on: 4 December 2024
Topic editor: Tony Robillard
Section editor: Enrico Schifani
Desk editor: Natacha Beau

Printed versions of all papers are deposited in the libraries of four of the institutes that are members of the *EJT* consortium: Muséum national d'Histoire naturelle, Paris, France; Meise Botanic Garden, Belgium; Royal Museum for Central Africa, Tervuren, Belgium; Royal Belgian Institute of Natural Sciences, Brussels, Belgium. The other members of the consortium are: Natural History Museum of Denmark, Copenhagen, Denmark; Naturalis Biodiversity Center, Leiden, the Netherlands; Museo Nacional de Ciencias Naturales-CSIC, Madrid, Spain; Leibniz Institute for the Analysis of Biodiversity Change, Bonn – Hamburg, Germany; National Museum of the Czech Republic, Prague, Czech Republic; The Steinhardt Museum of Natural History, Tel Aviv, Israël.

Supplementary files

Supp. file 1. Collection data for all material examined. https://doi.org/10.5852/ejt.2024.970.2757.12619
Supp. file 2. Measurement and index data for all material measured.
https://doi.org/10.5852/ejt.2024.970.2757.12623
Supp. file 3. Comparison of worker measurements between *Temnothorax ambiguus*, *T. caryaluteus* sp. nov., and *T. curvispinosus*. https://doi.org/10.5852/ejt.2024.970.2757.12625
Supp. file 4. Comparison of gyne measurements between *Temnothorax ambiguus*, *T. caryaluteus* sp. nov., and *T. curvispinosus*. https://doi.org/10.5852/ejt.2024.970.2757.12627